

Differentially Private Wireless Federated Learning Using Orthogonal Sequences

Xizixiang Wei Tianhao Wang Ruiquan Huang Cong Shen Jing Yang
H. Vincent Poor

Abstract

We propose a novel privacy-preserving uplink over-the-air computation (AirComp) method, termed FLORAS, for single-input single-output (SISO) wireless federated learning (FL) systems. From the communication design perspective, FLORAS eliminates the requirement of channel state information at the transmitters (CSIT) by leveraging the properties of orthogonal sequences. From the privacy perspective, we prove that FLORAS can offer both item-level and client-level differential privacy (DP) guarantees. Moreover, by adjusting the system parameters, FLORAS can flexibly achieve different DP levels at no additional cost. A novel FL convergence bound is derived which, combined with the privacy guarantees, allows for a smooth tradeoff between convergence rate and differential privacy levels. Numerical results demonstrate the advantages of FLORAS compared with the baseline AirComp method, and validate that our analytical results can guide the design of privacy-preserving FL with different tradeoff requirements on the model convergence and privacy levels.

Index Terms

Federated Learning; Differential Privacy; Convergence Analysis.

A preliminary version of this work will be presented at the 2023 IEEE International Conference on Communications [1].

Xizixiang Wei and Cong Shen are with the Charles L. Brown Department of Electrical and Computer Engineering, University of Virginia, USA. (E-mail: {xw8cw, cong}@virginia.edu).

Tianhao Wang is with the Department of Computer Science, University of Virginia, USA. (E-mail: tianhao@virginia.edu).

Ruiquan Huang and Jing Yang are with the Department of Electrical Engineering, the Pennsylvania State University, USA. (E-mail: {rzh5514, yangjing}@psu.edu).

H. Vincent Poor is with the Department of Electrical and Computer Engineering, Princeton University, USA. (E-mail: poor@princeton.edu).

I. INTRODUCTION

Real-world data generated or collected by edge devices enables various machine learning (ML) applications. For certain privacy-sensitive tasks, users prefer to keep their data locally instead of uploading it to cloud servers. Federated learning (FL) [2], [3] has emerged as a distributed ML paradigm that caters to this growing trend, and is able to train a global ML model across all local datasets without the server having direct access to client data.

The local training nature of FL leads to massive communication costs, as an FL task consists of multiple learning rounds, each of which requires uplink and downlink model exchange between clients and the server. Compared with downlink broadcasting, uplink communication is more challenging in FL. Due to the stringent power constraints at edge devices, channel noise and fading have a more conspicuous impact on uplink communications. More importantly, scalability of massively involved clients in FL versus limited uplink communication resources is highly challenging. Uplink communication is known as one of the key bottlenecks of wireless federated learning [4].

To tackle the scalability problem, over-the-air computation (also known as *AirComp*) mechanisms have been proposed (see [5] and the references therein). Instead of decoding individual local models of clients and then aggregating, AirComp allows multiple clients to transmit uplink signals in a natural superpositioned fashion over a wireless medium, and decodes the average global model directly at the FL server. AirComp dramatically improves the scalability of wireless FL, and naturally reduces the signal processing latency. Therefore, AirComp is regarded as a key technology for FL in future wireless networks and has been investigated extensively.

The most popular AirComp method is based on the channel inversion power control [6], which “inverts” the fading channel at each transmitter, so that the aggregated model can be directly obtained at the server. Variants and further enhancements of AirComp have been established and a detailed literature review can be found in Section II-A. Yet, a fundamental limitation of the existing methods is that they mostly require channel state information at the transmitters (CSIT). Enabling CSIT in communication systems is complicated and is substantially harder than obtaining the channel state information at the receivers (CSIR). Moreover, channel inversion based on CSIT is well known to “blow up” when one of the users’ channels is in deep fade [7]. Hence, exploring CSIT-free AirComp methods becomes attractive [8].

Meanwhile, with the ever-growing importance of data security, privacy preservation of client’s personal information has been increasingly valued by companies and governments. Although FL intuitively preserves clients’ privacy by keeping training data locally, private information can still be leaked to some extent by analyzing the differences of ML model parameters trained and uploaded by the clients [9]–[11].

To further address the privacy concern, a natural way is to add (artificial) noise to ML model parameters in the upload phase of FL, which can be mathematically characterized by differential privacy (DP) [12].

AirComp has the potential to achieve DP at no extra cost due to the nature-added noise in the wireless channel. Heuristically, different DP levels can be guaranteed by controlling the signal-to-noise ratio (SNR), and thus the effective channel noise level, at the receiver side. Yet, most of the literature on AirComp rarely characterizes achievable privacy protection in a mathematically rigorous fashion. A detailed review can be found in Section II-B. Moreover, we note that most literature focuses only on item-level DP in wireless FL, while client-level DP [13] is a new metric that is worth investigating.

To simultaneously remove the CSIT requirement of AirComp and address the privacy challenge, we propose FLORAS – Federated Learning using OrthogonAl Sequences, a novel uplink wireless physical layer design for FL by leveraging the properties of *orthogonal sequences*. On the communication design, FLORAS preserves all the advantages of AirComp while removing the CSIT requirement. From the perspective of privacy, FLORAS achieves desired DP guarantees (both item-level and client-level) by adjusting the number of used orthogonal sequences, making it much simpler and providing more flexibility to trade off privacy and utility.

The main contributions of this paper are summarized as follows:

- We proposed FLORAS for uplink communications in single-input single-output (SISO) wireless FL systems. FLORAS enjoys all the advantages of AirComp, yet without the CSIT requirement. In particular, orthogonal sequences allow the BS to obtain the individual CSIR via a single pilot, by which global ML model parameters can be estimated through simple linear projections. Therefore, FLORAS significantly reduces the channel estimation overhead. Different from the channel inversion power control, FLORAS allows the transmit power to be independent of the channel realizations, which avoids increasing the dynamic range of the transmit signal and improves the power efficiency.
- By adjusting the number of used orthogonal sequences in the system configuration, the novel signal processing technique in FLORAS produces Cauchy effective noise to the decoded global model, which empowers flexible item-level and client-level DP guarantees. Moreover, a new FL convergence bound based on truncated Cauchy noise is derived, which allows us to characterize the trade-off between the model convergence rate and the achievable DP levels.
- We conduct extensive experiments based on real-world datasets to evaluate the performance of FLORAS. Numerical results demonstrate the performance advantage of FLORAS compared with the channel inversion method and validate our theoretical analysis by demonstrating the trade-off between model convergence rate and DP level.

The remainder of this paper is organized as follows. Literature review is presented in Section II.

Section III introduces the FL pipeline and the uplink communication model. The proposed FLORAS design is detailed in Section IV. The DP guarantee and convergence analysis of FLORAS are presented in Section V and Section VI, respectively. Experimental results are reported in Section VII, followed by the conclusion of our work in Section VIII.

II. RELATED WORK

A. AirComp for FL

As a special case of computing over multiple access channels [14], AirComp [6], [15]–[17] leverages the signal superposition properties in a wireless multiple access channel to efficiently compute a sum/average function. This technique has attracted a lot of interest as it can reduce the uplink communication cost to be (nearly) agnostic to the number of participating clients. Client scheduling and various power and computation resource allocation methods have been investigated [18]–[23]. Full CSIT was relaxed in [24] by only using the phase information of the channel. Several studies have provided convergence guarantees of AirComp under different practical constraints and different types of heterogeneity [25]–[29]. In particular, [30], [31] propose CSIT-free AirComp methods leveraging channel orthogonality. However, they are effective only in massive MIMO systems.

B. Differential Privacy for FL

DP-SGD has been regarded as a standard framework to train a differentially private ML model [32]. Along with its variants [33], [34], recent years have also witnessed increased efforts on DP for distributed learning systems, including the clipping technique in [35], [36], the subsampling principle in [37], [38], and random quantization in [39], [40]. In the category of exploiting the channel noise for differentially private FL, [41] proposes an AirComp design to achieve certain DP by adjusting proper effective noise; [42], [43] investigate adding noise and power allocation in non-orthogonal multiple access (NOMA) systems; [44] explores it in multi-cell settings; [45] applies it to personalized FL. [46] jointly optimizes the latency and DP requirements of FL, and [47] discusses the trade-off among privacy, utility, and communication.

III. SYSTEM MODEL

A. FL Model

Consider an FL task with a central server and M clients. Each client $k \in [M]$ stores a (disjoint) local dataset \mathcal{D}_k , with its size denoted by D_k . The amount of the total data is $D \triangleq \sum_{k \in [M]} D_k$. We use $f_k(\mathbf{w})$

to denote the local loss function at client k , which measures how well an ML model with parameter $\mathbf{w} \in \mathbb{R}^d$ fits its local dataset. The global objective function over all M clients can be expressed as

$$f(\mathbf{w}) = \sum_{k \in [M]} p_k f_k(\mathbf{w}),$$

where $p_k = \frac{D_k}{D}$ is the weight for each local loss function, and the goal of FL is to find the optimal model parameter \mathbf{w}^* that minimizes the global loss function:

$$\mathbf{w}^* \triangleq \arg \min_{\mathbf{w} \in \mathbb{R}^d} f(\mathbf{w}).$$

We define $\Gamma \triangleq f^* - \sum_{k \in [M]} p_k f_k^*$ to capture the degree of the non-independent and identically distribution (non-IID) of local datasets, where f^* and f_k^* are the minima of global and local loss functions, respectively.

The FEDAVG framework [4] keeps client data locally, and the global model is obtained at the central server by the composition of multiple learning rounds. One of the key characteristics of FL is *partial clients participation*, i.e., only a portion of clients are selected in a single learning round for model upload. Here, we assume that K of total M clients are uniformly randomly selected during each learning round for the FL task. To simplify the notation, we use the subscript $k = 1, \dots, K$ to indicate the participating K clients during a certain learning round, acknowledging that they could correspond to different clients in different rounds.

A typical wireless FL pipeline iteratively executes the following steps in the t -th learning round.

- 1) **Downlink wireless communication.** The BS broadcasts the current global model \mathbf{w}_t to all K selected devices over the downlink wireless channel.
- 2) **Local computation.** Each client k uses its local data to train a local ML model \mathbf{w}_{t+1}^k improved upon the received global model \mathbf{w}_t . We assume that mini-batch stochastic gradient descent (SGD) is adopted to minimize the local loss function. The parameter is updated iteratively (for E steps) at client k as: $\mathbf{w}_{t,0}^k = \mathbf{w}_t$; $\mathbf{w}_{t,\tau}^k = \mathbf{w}_{t,\tau-1}^k - \eta_t \nabla \tilde{f}_k(\mathbf{w}_{t,\tau-1}^k, \xi_{t,\tau-1}^k), \forall \tau = 1, \dots, E$; $\mathbf{w}_{t+1}^k = \mathbf{w}_{t,E}^k$ where $\nabla \tilde{f}_k(\mathbf{w}, \xi)$ denotes the stochastic gradient at client k on model \mathbf{w} and mini-batch ξ .
- 3) **Uplink wireless communication.** Each involved client uploads its latest local model to the server synchronously over the uplink wireless channel.
- 4) **Server aggregation.** The BS aggregates the received noisy local models $\tilde{\mathbf{w}}_{t+1}^k$ to generate a new global model. For simplicity, we assume that each local dataset has an equal size; therefore we have $\mathbf{w}_{t+1} = \sum_{k=1}^K \frac{1}{K} \tilde{\mathbf{w}}_{t+1}^k$.

This work focuses on steps 3 and 4 in the FL pipeline. In particular, we leverage the unique properties of orthogonal sequences, which leads to an efficient FL uplink communication design with DP guarantees.

B. Communication Model

In each learning round, since there are K active clients, the uplink communication between clients and the central server can be modeled as over a (fading) multiple access channel. Consider a cell with a single-antenna BS and K single-antenna users involved in the FL task. The communication system leverages orthogonal sequences for uplink transmissions. Note that one of the most popular implementations of the orthogonal-sequence-based system is code-division multiple access (CDMA). We assume a spreading sequence set $\mathcal{A} = \{\mathbf{a}_1, \dots, \mathbf{a}_k, \dots, \mathbf{a}_N\}$ containing N unique spreading sequences ($N \geq K$), where each spreading sequence is denoted as $\mathbf{a}_k = [a_{1,k}, \dots, a_{L,k}]^T$ and L is the length of each spreading sequence. Each user is (randomly) assigned with a unique spreading sequence \mathbf{a}_k from \mathcal{A} as its signature.

We assume that the BS only has the knowledge of the entire spreading sequence set \mathcal{A} , *without knowing the specific signature of each user*. We emphasize that this restriction is consistent with our goal of guaranteeing user privacy – BS cannot identify users based on their spreading sequences or decode individual models. We will discuss the details of the spreading sequence assignment mechanism in Section V-D.

In the uplink communication, each client transmits the differential $\mathbf{x}_t^k \triangleq [x_{1,t}^k, \dots, x_{i,t}^k, \dots, x_{d,t}^k]^T \in \mathbb{R}^d$ between the received global model and the computed new local model:

$$\mathbf{x}_t^k = \mathbf{w}_t - \mathbf{w}_{t+1}^k, \quad \forall k = 1, \dots, K,$$

to the BS, whose objective is to estimate $\mathbf{x}_t \triangleq \sum_{k=1}^K \mathbf{x}_t^k$.

Before the transmission of model differential \mathbf{x}_t^k , we assume that the BS will use the following normalization technique to ensure $\mathbb{E}[\mathbf{x}_t^k] = 0$ and $\|\mathbf{x}_t^k\|_2^2 = C^2$:

$$\mathbf{x}_t^k \leftarrow \frac{C(\mathbf{x}_t^k - \mu)}{\|\mathbf{x}_t^k - \mu\|_2},$$

where $\mu \triangleq \frac{1}{d} \sum_{i=1}^d x_{i,t}^k$ is the sample mean of \mathbf{x}_t^k . Note that normalization parameters μ and $C/\|\mathbf{x}_t^k - \mu\|_2$ will be sent to the BS via a separate control channel as suggested in [6] for the de-normalization. The l_2 -norm term in the normalization not only guarantees the sensitivity of \mathbf{x}_t^k for the DP analysis in Section V, but also satisfies the practical requirement that each client has a limited energy budget for transmission of the model differential in a single round. We note that similar technique has also been applied in [35].

To simplify the notation, we omit index t and use x_k^i instead of $x_{i,t}^k$ barring any confusion. We assume that each client transmits every element of the differential model $\{x_k^1, \dots, x_k^d\}$ via d shared time slots. In addition, *block fading channel* is assumed¹, i.e., the fading channel between each client and the BS

¹The large-scale pathloss and shadowing effect is assumed to be taken care of by, e.g., open loop power control [48].

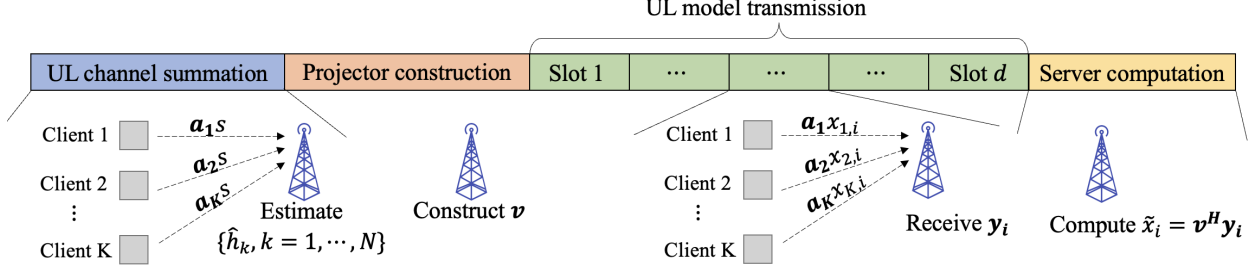


Fig. 1. Illustration of the proposed uplink communication design of FLORAS.

h_k remains unchanged in d time slots. We emphasize that we do not make any specific assumption on the fading distribution throughout this paper. In the i -th slot, each client transmits symbol x_k^i spread by its uniquely assigned orthogonal sequence. The BS received signal can be written as

$$\mathbf{y}_i = \sum_{k=1}^K \mathbf{a}_k h_k x_k^i + \mathbf{n}_i \quad \forall i = 1, \dots, d,$$

where \mathbf{n}_i is the additive white Gaussian noise (AWGN) with mean zero and variance σ^2/L per dimension. Note that since the global model differential parameters are real signals, we only need to consider the real part of channel coefficients and noise here. Although one-dimensional (real) modulation cannot fully leverage the channel degrees of freedom, it is consistent with the fact that binary phase-shift keying (BPSK) is the most common modulation scheme in CDMA systems [7]. In addition, focusing on the real dimension makes the subsequent discussion easier and highlights our contribution better. Also, as we detail later in Remark 2, we can leverage full channel gain at an affordable cost of partial CSIT.

We note that spreading sequences are *orthonormal*, i.e.,

$$\mathbf{a}_i^T \mathbf{a}_i = 1, \quad \forall i; \quad \text{and} \quad \mathbf{a}_i^T \mathbf{a}_j = 0, \quad \forall i \neq j. \quad (1)$$

At the BS, the receiver will decode the estimated aggregation parameter \tilde{x}_i , which is a noisy version of $x_i \triangleq \sum_{k=1}^K x_k^i$, and recover $\tilde{\mathbf{x}}_t \triangleq [\tilde{x}_1, \dots, \tilde{x}_d]^T$ in d slots. After that, the BS can compute the new global model as

$$\mathbf{w}_{t+1} = \mathbf{w}_t + \frac{1}{K} \tilde{\mathbf{x}}_t. \quad (2)$$

Throughout the paper, we assume that all users are synchronized in frames, which can be achieved by the BS sending a beacon signal to initialize uplink transmissions [48].

IV. FLORAS

In this section, we present the design of FLORAS for uplink communications in wireless FL.

A. Algorithm Design

FLORAS is a four-step framework and each step is detailed as follows.

Step 1: Uplink channel estimation. Before the model differential transmission, the BS schedules *all* participating users to transmit a common pilot s simultaneously. The received signal is

$$\mathbf{y}_s = \sum_{k=1}^K \mathbf{a}_k h_k s + \mathbf{n}_s.$$

The BS can utilize \mathbf{y}_s and the complete set of orthogonal sequences $\mathcal{A} = \{\mathbf{a}_1, \dots, \mathbf{a}_N\}$ to estimate the channel gain coefficients. For the K spreading sequences that are actually adopted by the user², we have

$$\hat{h}_k = \frac{\mathbf{a}_k^T \left[\sum_{i=1}^K \mathbf{a}_i h_i s + \mathbf{n}_s \right]}{s} = h_k + \frac{\mathbf{a}_k^T \mathbf{n}_s}{s}, \forall k = 1, \dots, K.$$

For the last $N - K$ spreading sequences that are not selected by any user, the BS obtains

$$\hat{h}_k = \frac{\mathbf{a}_k^T \left[\sum_{i=1}^K \mathbf{a}_i h_i s + \mathbf{n}_s \right]}{s} = \frac{\mathbf{a}_k^T \mathbf{n}_s}{s}, \forall k = K + 1, \dots, N.$$

Step 2: Projector construction. For simplicity, we assume $s = 1$ in the following discussion. After the channel estimation, the BS constructs the following vector based on *all of* the estimated channel coefficients:

$$\mathbf{v} = \sum_{k=1}^N \frac{1}{\hat{h}_k} \mathbf{a}_k = \sum_{k=1}^K \frac{\mathbf{a}_k}{h_k + \mathbf{a}_k^T \mathbf{n}_s} + \sum_{k=K+1}^N \frac{\mathbf{a}_k}{\mathbf{a}_k^T \mathbf{n}_s}.$$

We note that since the BS does not know which K of the total N spreading sequences are adopted by the users, it has to use all of $\{\hat{h}_1, \dots, \hat{h}_N\}$ to construct the projector \mathbf{h}_s . This seemingly redundant design actually enables better privacy protection, which will be clear in Section V.

Step 3: UL model transmission. All users upload every element of the differentials via d shared time slots:

$$\mathbf{y}_i = \sum_{k=1}^K \mathbf{a}_k h_k x_k^i + \mathbf{n}_i, \quad \forall i = 1, \dots, d.$$

Step 4: Sum model decoding. The BS applies the following linear projection to estimate each aggregated model differential $x_i, \forall i = 1, \dots, d$:

$$\tilde{x}_i = \mathbf{v}^T \mathbf{y}_i = \sum_{k=1}^N \frac{1}{\hat{h}_k} \mathbf{a}_k \left[\sum_{k=1}^K \mathbf{a}_k h_k x_k^i + \mathbf{n}_i \right]$$

²Without loss of generality, we assume the first K spreading sequences from the set are selected. This assumption is made to ease the notation.

$$\begin{aligned}
&= \left[\sum_{k=1}^K \frac{\mathbf{a}_k}{h_k + \mathbf{a}_k^T \mathbf{n}_s} + \sum_{k=K+1}^N \frac{\mathbf{a}_k}{\mathbf{a}_k^T \mathbf{n}_s} \right] \left[\sum_{k=1}^K \mathbf{a}_k h_k x_k^i + \mathbf{n}_i \right] \\
&= \sum_{k=1}^K \frac{h_k}{h_k + \mathbf{a}_k^T \mathbf{n}_s} x_k^i + \sum_{k=1}^K \frac{\mathbf{a}_k^T \mathbf{n}_i}{h_k + \mathbf{a}_k^T \mathbf{n}_s} + \sum_{k=K+1}^N \frac{\mathbf{a}_k^T \mathbf{n}_i}{\mathbf{a}_k^T \mathbf{n}_s}.
\end{aligned}$$

After decoding $\{\tilde{x}_1, \dots, \tilde{x}_d\}$, the BS can compute the new global model following (2) and start the next learning round. The above four-step procedure is illustrated in Fig. 1.

B. Preliminary Analysis

In the high signal-to-noise ratio (SNR) regime, where the channel fading effect dominates the noise, we have $\mathbb{E}[\|\mathbf{a}_k^T \mathbf{n}_s\|^2] \ll \mathbb{E}[\|h_k\|^2]$. Therefore, we can establish the following approximation for the estimated model in Step 4:

$$\tilde{x}_i \approx \sum_{k=1}^K x_k^i + \sum_{k=K+1}^N \frac{\mathbf{a}_k^T \mathbf{n}_i}{\mathbf{a}_k^T \mathbf{n}_s}, \quad \forall i = 1, \dots, d, \quad (3)$$

where $\sum_{k=K+1}^N \frac{\mathbf{a}_k^T \mathbf{n}_i}{\mathbf{a}_k^T \mathbf{n}_s}$ denotes the dominant noise of the received global model parameters³. The distribution of this post-processing noise is not straightforward, and we next present Lemma 1 to establish that the noise term is a *Cauchy random variable*.

Lemma 1. For IID Gaussian random vector $\mathbf{n}_i, \mathbf{n}_s \sim \mathcal{N}(0, \frac{\sigma^2}{L} \mathbf{I})$, random variable

$$X \triangleq \sum_{k=K+1}^N \frac{\mathbf{a}_k^T \mathbf{n}_i}{\mathbf{a}_k^T \mathbf{n}_s} \sim \text{Cauchy}(0, N - K), \quad \forall \mathbf{a}_k \in \mathcal{A},$$

with probability density function (PDF)

$$f_X(x) = \frac{1}{\pi} \frac{N - K}{x^2 + (N - K)^2}, \quad x \in \mathbb{R}.$$

Proof. We first note that $\mathbf{a}_k^T \mathbf{n}_i$ and $\mathbf{a}_k^T \mathbf{n}_s$ are Gaussian random variables since they are linear combinations of IID Gaussian random variables. Let

$$Y \triangleq [\mathbf{a}_{K+1}^T \mathbf{n}_i, \mathbf{a}_{K+2}^T \mathbf{n}_i, \dots, \mathbf{a}_N^T \mathbf{n}_i]^T,$$

and

$$Z \triangleq [\mathbf{a}_{K+1}^T \mathbf{n}_s, \mathbf{a}_{K+2}^T \mathbf{n}_s, \dots, \mathbf{a}_N^T \mathbf{n}_s]^T.$$

³Note that this approximation drops the minor noise term, which results in that the DP guarantee in the later discussion is the lower bound of the actual DP level of FLORAS.

It is straightforward to verify that Y and Z are IID Gaussian random vectors with distribution $\mathcal{N}(0, \Sigma)$, where Σ is a covariance matrix. According to [49], we have

$$\sum_{k=K+1}^N w_k \frac{Y_k}{Z_k} = \sum_{k=K+1}^N b_k \frac{\mathbf{a}_k^T \mathbf{n}_i}{\mathbf{a}_k^T \mathbf{n}_s} \sim \text{Cauchy}(0, 1),$$

as long as w_k is independent from (Y, Z) and $\sum_{k=K+1}^N w_k = 1$. Let $b_k = \frac{1}{N-K}$ and based on the fact that $kX \sim \text{Cauchy}(0, |k|)$ if $X \sim \text{Cauchy}(0, 1)$, we prove Lemma 1. \square

Cauchy distribution is known as a “fat tail” distribution, as the tail of its PDF decreases proportionally with $1/x^2$. Lemma 1 suggests that, for a fixed K , a larger spreading sequence set will result in a heavier tail in the Cauchy noise. Therefore, we can adjust the size of the spreading sequence set to induce different additive Cauchy noise in (3). We will discuss the effect of different Cauchy noise on DP and convergence in Sections V and VI, respectively.

A few remarks about FLORAS are now in order.

Remark 1 (Advantages over the channel inversion method). *Compared with the widely investigated channel inversion-based AirComp design, FLORAS does not require CSIT for uplink communications, which greatly reduces the communication overhead. This is especially attractive for Internet-of-Things (IoT) applications with massive devices. Moreover, in SISO systems, the maximum uplink transmit power of each user in the channel inversion-based methods is usually limited by the worst channel gain, and the received SNR of the global model and the efficiency of power amplifiers (PAs) will significantly decrease, if one of the client channels experiences deep fading [7]. Thanks to the orthogonality of spreading sequences, FLORAS allows the transmit power to be independent of channel realizations, and thus avoids increasing the dynamic range of the transmit signal, which dramatically improves the power efficiency of PAs.*

Remark 2 (Leverage full channel degrees of freedom). *As mentioned before, real modulation cannot leverage full degrees of freedom of complex channel h_k . To address this limitation, we can borrow the idea of [50]. Specifically, the fading channel between each client and the BS can be written as*

$$h_k = \tilde{h}_k e^{j\phi_k}, \quad \forall k = 1, \dots, K,$$

where $\tilde{h}_k \triangleq |h_k| \in \mathbb{R}_+$ and $\phi_k \triangleq \angle h_k \in [0, 2\pi)$ represent channel amplitude/gain and phase, respectively. For a given x_k^i , client k transmits symbol $x_k^i e^{-j\phi_k}$, where $e^{-j\phi_k}$ is the phase correction term as suggested

in [50]. Hence the received signal at the BS can be written as

$$\mathbf{y}_i = \sum_{k=1}^K \mathbf{a}_k h_k e^{-j\phi_k} x_k^i + \mathbf{n}_i = \sum_{k=1}^K \mathbf{a}_k \tilde{h}_k x_k^i + \mathbf{n}_i, \forall i = 1, \dots, d.$$

By phase correction, the imaginary part of h_k is projected to the real domain and the full channel gain can be leveraged without losing any other advantages of FLORAS. We note that just as in [50], this approach requires each client k to have the channel phase information ϕ_k , which is weaker than requiring the complete CSIT h_k but stronger than the standard FLORAS.

Remark 3 (Extensions on NOMA systems). Another limitation of FLORAS is that the number of orthogonal spreading sequences is fixed for a given sequence length. To involve more clients during a learning round, or to expand the size of set \mathcal{A} , the system would need to adopt longer spreading sequences, which consumes more bandwidth. We first note that although there may exist a massive number of clients in an FL task, the number of involved clients in each learning round is usually relatively small (due to client selection), which implies the bandwidth cost is affordable for our design. Secondly, as an alternative, the system can adopt a non-orthogonal spreading sequence to improve the scalability without the cost of extra bandwidth. Applying a non-orthogonal spreading sequence is consistent with non-orthogonal multiple access (NOMA) systems, which is an emerging technology for massive machine-type communications (mMTC) applications. For non-orthogonal spreading sequence, the requirement of spreading sequence in (1) becomes

$$\mathbb{E} [\mathbf{a}_i^T \mathbf{a}_i] = 1, \quad \forall i \quad \text{and} \quad \mathbb{E} [\mathbf{a}_i^T \mathbf{a}_j] = 0, \quad \forall i \neq j,$$

which can be achieved by random Gaussian vectors. Note that Lemma 1 still holds for non-orthogonal spreading sequences, since it allows an arbitrary covariance matrix of random Gaussian vector Y and Z . Non-orthogonal spreading sequences will introduce inter-symbol interference besides noise when decoding global model parameters in Step 4. Therefore, the convergence bound proposed in Section VI can be regarded as a lower bound for NOMA systems. For more analysis in the presence of interference, readers can refer to [51].

V. DIFFERENTIAL PRIVACY

In this section, we analyze the DP level achieved by FLORAS. We begin by introducing the basic concepts of DP in FL, and then prove that FLORAS achieves different levels of DP via the adjustment of the size of spreading sequence set N and the number of involved clients K . Both item-level and client-level DP are analyzed. The DP guarantee not only considers multiple sources of randomness in

wireless FL, including random mini-batch in SGD and Cauchy noise, but also reveals the influence on multiple learning rounds.

A. Preliminaries

To formalize the definition of DP, we first introduce the concept of *neighboring datasets*. We say that two datasets \mathcal{D} and \mathcal{D}' are neighboring, written as $\mathcal{D} \sim \mathcal{D}'$, if they differ in at most one sample.

Based on this concept, we state the standard definition of (ϵ, δ) -DP as follows.

Definition 1 ((ϵ, δ) -DP [12]). *A randomized algorithm $\mathcal{M} : X^n \rightarrow \mathcal{R}$ provides (ϵ, δ) -DP with $0 < \delta < 1$, if for all pairs of neighboring datasets $\mathcal{D} \sim \mathcal{D}'$ and all (measurable) sets of outcomes $S \subseteq \mathcal{R}$, we have*

$$\mathbb{P}[\mathcal{M}(\mathcal{D}) \in S] \leq e^\epsilon \mathbb{P}[\mathcal{M}(\mathcal{D}') \in S] + \delta.$$

We say that a random algorithm is ϵ -DP (also known as *pure DP*), if it satisfies (ϵ, δ) -DP with $\delta = 0$. The common interpretation of δ in (ϵ, δ) -DP is the “leakage probability”, i.e., (ϵ, δ) -DP is ϵ -DP “except with probability δ ”.

We next introduce the definition of Rényi DP [52]. As a generalization of (ϵ, δ) -DP, it can help us obtain a tighter (ϵ, δ) -DP bound converted from its composition, which is particularly attractive in FL due to multiple learning rounds.

Definition 2 ((α, ϵ) -Rényi DP [52]). *A randomized algorithm $\mathcal{M} : X^n \rightarrow \mathcal{R}$ is said to provide (α, ϵ) -Rényi DP, if for any pair of neighboring datasets $\mathcal{D} \sim \mathcal{D}'$ it holds that*

$$D_\alpha(\mathcal{M}(\mathcal{D}) || \mathcal{M}(\mathcal{D}')) \leq \epsilon,$$

where

$$D_\alpha(\mathcal{M}(\mathcal{D}) || \mathcal{M}(\mathcal{D}')) \triangleq \frac{1}{\alpha - 1} \log \int_{-\infty}^{+\infty} P(x)^\alpha Q(x)^{1-\alpha} dx$$

is the Rényi divergence. Specially, for $\alpha = +\infty$, we have

$$D_\infty(\mathcal{M}(\mathcal{D}) || \mathcal{M}(\mathcal{D}')) = \sup_{x \in \text{supp} Q} \log \frac{P(x)}{Q(x)}.$$

In the AirComp FL design, decoding the global model from the received signal can be regarded as a randomized mechanism on $\mathcal{D} = \bigcup_{k=1}^K \mathcal{D}_k$, where \mathcal{D} is the union of the local datasets of all the participated K clients per learning round. We denote this randomized mechanism as

$$\mathcal{M}(\mathcal{D}) \triangleq \tilde{\mathbf{x}}_t = g(\mathcal{D}) + \mathbf{n}_t, \quad (4)$$

where $g(\mathcal{D}) = \mathbf{x}_t = \sum_{k=1}^K \mathbf{x}_t^k$ the noise-free summation of model differentials, and \mathbf{n}_t is a random noise following a certain distribution. The randomness of the mechanism comes from the random mini-batch in SGD when calculating \mathbf{x}_t^k and the random noise.

To determine the DP level, we next define the *global sensitivity function* for operation $g(\cdot)$ as

$$GS_g = \max_{\mathcal{D}, \mathcal{D}'} \|g(\mathcal{D}) - g(\mathcal{D}')\|_2, \quad (5)$$

where \mathcal{D}' is a neighboring dataset of \mathcal{D} . As mentioned in Section III, for uplink communication, we ensure that $\|\mathbf{x}_t^k\|_2 \leq C$. Therefore, we have

$$\begin{aligned} GS_g &= \max_{\mathcal{D}, \mathcal{D}'} \|g(\mathcal{D}) - g(\mathcal{D}')\|_2 = \max_{\mathbf{x}_t^k, \mathbf{x}_t^{k'}} \|\mathbf{x}_t^k - \mathbf{x}_t^{k'}\|_2 \\ &\leq \max_{\mathbf{x}_t^k, \mathbf{x}_t^{k'}} [\|\mathbf{x}_t^k\|_2 + \|\mathbf{x}_t^{k'}\|_2] \leq 2C, \end{aligned} \quad (6)$$

where $\mathbf{x}_t^{k'}$ denotes the noise-free model differential from client k' whose local dataset is swapped in a random data sample.

B. Item-level Differential Privacy

We proceed to derive the Rényi DP of FLORAS. It is worth mentioning that our analyses consider the DP not only from the Cauchy noise, but also from the random mini-batch SGD operation in the local updates of each learning round.

Theorem 1. *Given a spreading sequence set \mathcal{A} containing N unique sequences and M clients involved in an FL task. In each learning round, K ($K < N$) clients are randomly selected for model updates. With local dataset \mathcal{D}_k of size D_k and mini-batch size d_k ($d_k < D_k$), FLORAS provides (α, ϵ) -Rényi DP for the global model, where*

$$\epsilon = \frac{1}{2} \alpha \log^2 \left(1 + \frac{4qC^2}{(N-K)^2} \right) = O \left(\frac{\alpha q^2 C^4}{(N-K)^4} \right), \quad (7)$$

and $q \triangleq \frac{d_k}{D_k}$.

Proof. See Appendix A-B. □

Based on the composition rule of Rényi DP, we next establish the (ϵ, δ) -DP guarantee for the overall uplink communications in an FL task of T rounds.

Theorem 2. Consider a wireless FL task with T learning rounds, a spreading sequence set \mathcal{A} containing N unique sequences, and K clients ($K < N$). With local dataset \mathcal{D}_k of size D_k and mini-batch size d_k ($d_k < D_k$), FLORAS provides (ϵ', δ) -DP for the entire FL task, where

$$\begin{aligned} \epsilon' &= \sqrt{2T \log(1/\delta)} \log \left(1 + \frac{4qC^2}{(N-K)^2} \right) \\ &+ \frac{1}{2}T \log^2 \left(1 + \frac{4qC^2}{(N-K)^2} \right) \sim \tilde{O} \left(\frac{\sqrt{T}q}{(N-K)^2} \right). \end{aligned} \quad (8)$$

Proof. See Appendix A-C. □

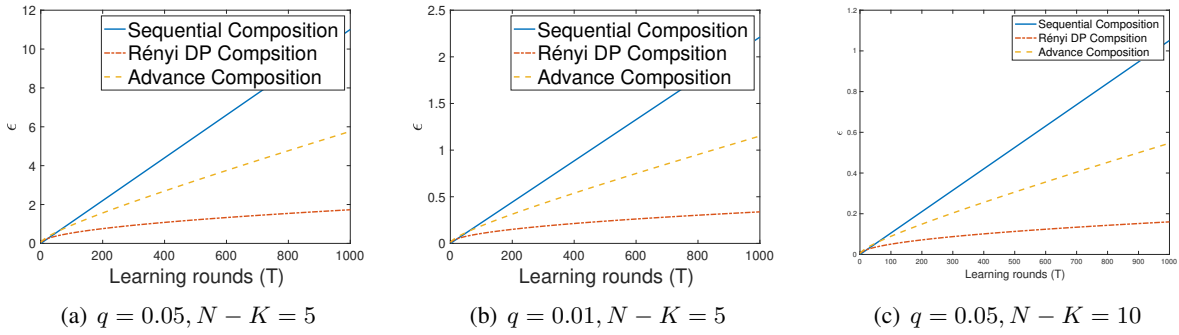


Fig. 2. Comparison of sequential composition, Rényi DP composition, and advanced composition with different sizes of mini-batch SGD and orthogonal sequence set.

Theorems 1 and 2 reveal that, for a fixed FL configuration, i.e., fixed number of selected clients K , mini-batch size rate q , and the number of learning rounds T , the expansion of spreading sequence set would achieve a higher level of DP per learning round and for the whole learning task, respectively. In particular, $\epsilon \propto \frac{1}{(N-K)^4}$ in Rényi DP for each learning round, and $\epsilon' \propto \frac{1}{(N-K)^2}$ in (ϵ, δ) -DP for the whole learning task. Since the BS (adversary) has no knowledge of which particular K out of the total N spreading sequences the clients have chosen, increasing the number of spreading sequences results in a heavier tail of the post-processing Cauchy noise, which achieves better privacy protection.

Guided by Theorem 2, we can adjust N to meet the privacy requirement of a practical FL task. Note that larger noise (better privacy protection) will affect the convergence rate of FL, and we will discuss this impact in detail in Section VI.

Remark 4 (Choice of DP metrics). Note that we use (ϵ, δ) -DP to evaluate the overall DP guarantee of the FL task. The reason why we choose to utilize Rényi DP to analyze the DP guarantee per learning round is the same as [53]: we can obtain a tighter (ϵ, δ) -DP guarantee from the composition of multiple Rényi-DP mechanisms. This advantage is empirically shown in Fig. 2, in which we compare the overall DP

guarantees v.s. learning rounds of three different composition methods: i) vanilla sequential composition of (ϵ, δ) -DP; ii) advanced composition of (ϵ, δ) -DP; iii) (ϵ, δ) -DP converted from composition of Rényi DP. It clearly demonstrates that under different system configurations, Theorem 2 unanimously provides the tightest (ϵ, δ) -DP guarantee, which is consistent with the theoretical and experimental results in [52].

Remark 5 (Trade-off between privacy and bandwidth). Note that for spreading sequences of length L , there are at most L unique spreading sequences. In a spreading spectrum system, bandwidth is proportional to the length of the spreading sequence. Hence, achieving a certain DP level via N spreading sequences in \mathcal{A} will consume $\rho = \frac{N}{K} - 1$ extra relative bandwidth compared with the non-DP case ($N = K$). Substituting ρ into Eqn. (8) leads to an expression of ϵ' that scales as $\tilde{O}\left(\frac{1}{\rho^2}\right)$, which provides a principled approach to balance DP levels and system bandwidth in a practical system.

C. Client-level Differential Privacy

So far, we have focused on the standard item-level DP that protects a single data sample of a certain local dataset. For FL, another DP concept called *client-level DP* (also known as user-level DP) is also important. Client-level DP protects data from a single client, which requires that the server cannot identify the participation of one client by observing the received signals.

The definition of client-level DP follows similarly from Definition 1, with a slight change that the neighboring dataset pair $\mathcal{D} \sim \mathcal{D}'$ differs in at most the data samples of one single client. As a result, client-level DP protects privacy when the entire data from a certain client is swapped. From the previous discussion of global sensitivity, the output \mathbf{x}_t^k is always bounded even though the entire dataset of a certain client changes. Therefore, our method naturally satisfies the client-level DP and we formally establish the corresponding guarantee.

Theorem 3. Given a spreading sequence set \mathcal{A} containing N unique sequences and K clients involved in an FL task, in each learning round, FLORAS provides (α, ϵ) -client level Rényi DP, where

$$\epsilon = \frac{1}{2}\alpha \log^2 \left(1 + \frac{4C^2}{(N-K)^2} \right) = O \left(\frac{\alpha C^4}{(N-K)^4} \right). \quad (9)$$

Moreover, for total T learning rounds, FLORAS provides (ϵ'', δ) -client level DP for the entire FL task, where

$$\begin{aligned} \epsilon'' &= \sqrt{2T \log(1/\delta)} \log \left(1 + \frac{4C^2}{(N-K)^2} \right) \\ &+ \frac{1}{2}T \log^2 \left(1 + \frac{4C^2}{(N-K)^2} \right) \sim \tilde{O} \left(\frac{\sqrt{T}}{(N-K)^2} \right) \end{aligned} \quad (10)$$

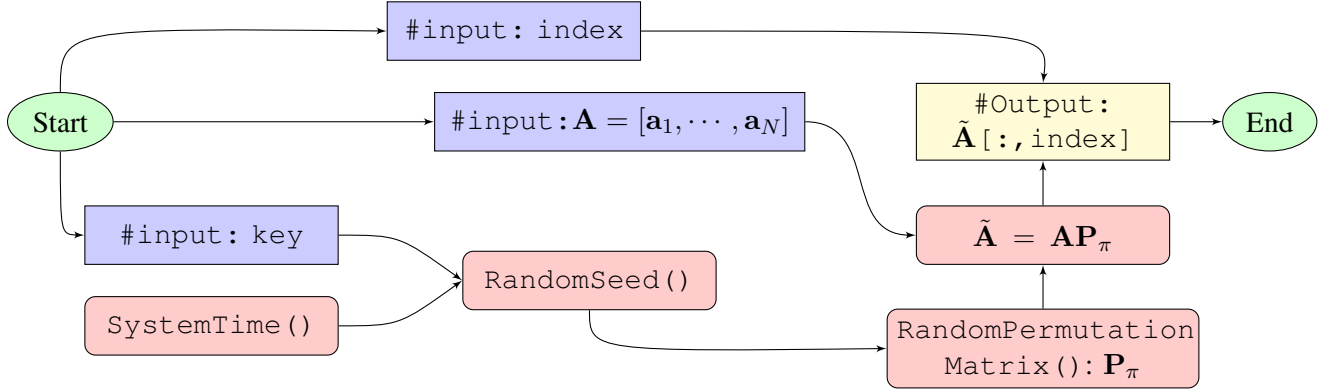


Fig. 3. Flowchart of the designed spreading sequence assignment mechanism for any given client.

Proof. See Appendix A-D. □

Theorem 3 demonstrates that FLORAS provides the client-level DP guarantee in a manner that is similar to the item-level DP. However, since the entire local dataset of a certain client would be swapped, we cannot take advantage of the SGD randomness in the analysis of client-level DP. Therefore, q disappears from the client-level DP guarantee.

D. Spreading Sequence Assignment Mechanism

As we have discussed, the DP guarantee of FLORAS comes from the fact that the assignment of spreading sequences remains unknown to the BS (adversary). In traditional CDMA systems, the spreading sequence is assigned to each device by the BS. This mechanism becomes invalid in our setting, since we need to make sure that the BS only has the knowledge of the spreading sequence set \mathcal{A} , not the individual assignment. In practice, we can resort to a trusted third-party to handle the assignment of orthogonal sequences. The design of such a mechanism belongs to the field of *secure multi-party computation (MPC)* [54], [55] and is out of the scope of this paper.

In the following, we provide a preliminary reference design based on a random permutation algorithm as illustrated in Fig. 3. The proposed design allows each user to autonomously choose a unique spreading code without collision. To better explain the mechanism, we first define a *fixed* matrix based on $\mathcal{A} = \{\mathbf{a}_k, k = 1, \dots, N\} : \mathbf{A} = [\mathbf{a}_1, \dots, \mathbf{a}_N] \in \mathbb{R}^{L \times N}$. We assume that every device that will be involved in the FL task shares a common confidential `key`. This key is *a priori* knowledge to clients, yet confidential to the BS (adversary). This assumption can be achieved via standard cryptography approaches, e.g., the key-exchange protocol [56]. When the BS schedules clients to participate in the current learning round, an `index` $\in \{1, \dots, K\}$ will be assigned to each client. After that, every client leverages the confidential

Key and the current system time `SystemTime()` to generate a random seed `RandSeed()`. Since the system has been synchronized, each client will obtain the same random seed, and generate a (common) random permutation matrix $\mathbf{P}_\pi \in \mathbb{R}^{N \times N}$ based on that. Followed by a random column permutation $\tilde{\mathbf{A}} = \mathbf{A}\mathbf{P}_\pi$, each client can use the `index`-th column $\tilde{\mathbf{A}}[:, \text{index}]$ as its spreading sequence for the current learning round. Note that as long as the confidential key is not leaked, the BS (adversary) will not know which K of the total N spreading sequences are adopted in the current learning round.

Remark 6. We emphasize that the established DP guarantee is for the receiver processing proposed in Section IV-A. There may exist more sophisticated receiver algorithms, which could conceivably attempt to infer more information about the usage of the orthogonal sequences per learning round from the received signal. However, since we do not make any assumptions on the channel distribution, such approach would be difficult in general. Besides, it is impossible to always accurately identify all used sequences due to the channel noise. Therefore, even under this scenario, the proposed framework still provides privacy, although the DP guarantee dependency may decrease from $O(1/(N - K))$ to $O(1/\alpha(N - K))$, where $0 < \alpha < 1$.

VI. CONVERGENCE ANALYSIS

We analyze the convergence behavior of FLORAS in this section. We first make the following standard assumptions that are commonly adopted in the convergence analysis of FEDAVG and its variants; see [57]–[60].

Assumption 1. L -smooth: $\forall \mathbf{v}$ and \mathbf{w} , $\|f_k(\mathbf{v}) - f_k(\mathbf{w})\| \leq L \|\mathbf{v} - \mathbf{w}\|$;

Assumption 2. μ -strongly convex: $\forall \mathbf{v}$ and \mathbf{w} , $\langle f_k(\mathbf{v}) - f_k(\mathbf{w}), \mathbf{v} - \mathbf{w} \rangle \geq \mu \|\mathbf{v} - \mathbf{w}\|^2$;

Assumption 3. Unbiased SGD: $\forall k \in [M]$, $\mathbb{E}[\nabla \tilde{f}_k(\mathbf{w})] = \nabla f_k(\mathbf{w})$;

Assumption 4. Uniformly bounded gradient: $\forall k \in [M]$, $\mathbb{E} \left\| \nabla \tilde{f}_k(\mathbf{w}) \right\|^2 \leq H^2$ for all mini-batch data.

We notice that a Cauchy distribution has uncertain (infinity) variance, which brings a significant challenge to the convergence analysis as the noise variance cannot be bounded. To address this issue, we assume the BS applies a *truncation* operation in the interval $[-B, B]$ on the decoded global parameters in (3):

$$\tilde{x}_i \approx \max \left(\min \left(\sum_{k=1}^K x_k^i + \sum_{k=K+1}^N \frac{\mathbf{a}_k^T \mathbf{n}_i}{\mathbf{a}_k^T \mathbf{n}_s}, B \right), -B \right) \quad (11)$$

where $B \gg C$. Note that the truncation operation is universal (albeit sometimes implicit) in almost all practical systems, since the signal values in the processing units are always finite. As long as we ensure $B \gg C$, the truncation operation has very little impact on the received signal. For ease of exposition, we make the following assumption on the noise term in (11).

Assumption 5. *The noise term in (11) follows a truncated Cauchy distribution within the interval $[-B, B]$ with $B \gg C$, whose PDF can be expressed as*

$$f_X(x) = \frac{1}{2 \arctan\left(\frac{B}{N-K}\right)} \frac{N-K}{x^2 + (N-K)^2}, x \in [-B, B].$$

We note that Assumption 5 becomes more accurate as the gap between B and C increases. Also note that the DP guarantee of FLORAS in Section V still holds under Assumption 5. We next establish Theorem 4 as the convergence guarantee of FLORAS.

Theorem 4. *With Assumptions 1-5, for some $\gamma \geq 0$, if we select the learning rate as $\eta_t = \frac{2}{\mu(t+\gamma)}$, a wireless system implementing the proposed design for FL uplink communication achieves*

$$\mathbb{E}[f(\mathbf{w}_t)] - f^* \leq \frac{L}{2(t+\gamma)} \left[\frac{4G}{\mu^2} + (1+\gamma) \|\mathbf{w}_0 - \mathbf{w}^*\|^2 \right],$$

for any $t \geq 1$, where

$$G = \sum_{k=1}^M \frac{H_k^2}{M^2} + 6L\Gamma + 8(E-1)^2 H^2 + \frac{M-K}{M-1} \frac{4}{K} \eta_t^2 E^2 H^2 + D(\epsilon).$$

and

$$D(\epsilon) = \frac{64}{K^2 \epsilon^2 \arctan\left(\frac{B\epsilon}{4C}\right)} \left[\frac{B\epsilon}{4C} - \arctan\left(\frac{B\epsilon}{4C}\right) \right] E^2 H^2.$$

Proof. See Appendix B. □

Theorem 4 demonstrates that FLORAS preserves the $O(1/T)$ convergence rate of SGD for strongly convex loss functions (compared with the noise-free FL convergence). For a fixed initial point, there are multiple factors in the constant B that affect the convergence rate of FL. In particular, $\sum_{k=1}^K \frac{H_k^2}{K^2}$ reveals the *variance reduction* effect of SGD by involving more clients. $6L\Gamma$ and $8(E-1)^2 H^2$ capture the influence of non-IID dataset and the number of local epochs, respectively. The last term $D(\epsilon)$ in B demonstrates the impact from Cauchy noise, i.e. level of privacy protection. We note that $D(\epsilon)$ is increasing as ϵ gets closer to 0. It implies that a higher level of privacy protection will decrease the speed of convergence as constant B becomes larger. Therefore, Theorem 4 establishes a trade-off between privacy protection and convergence rate, which provides guidance for the practical system design.

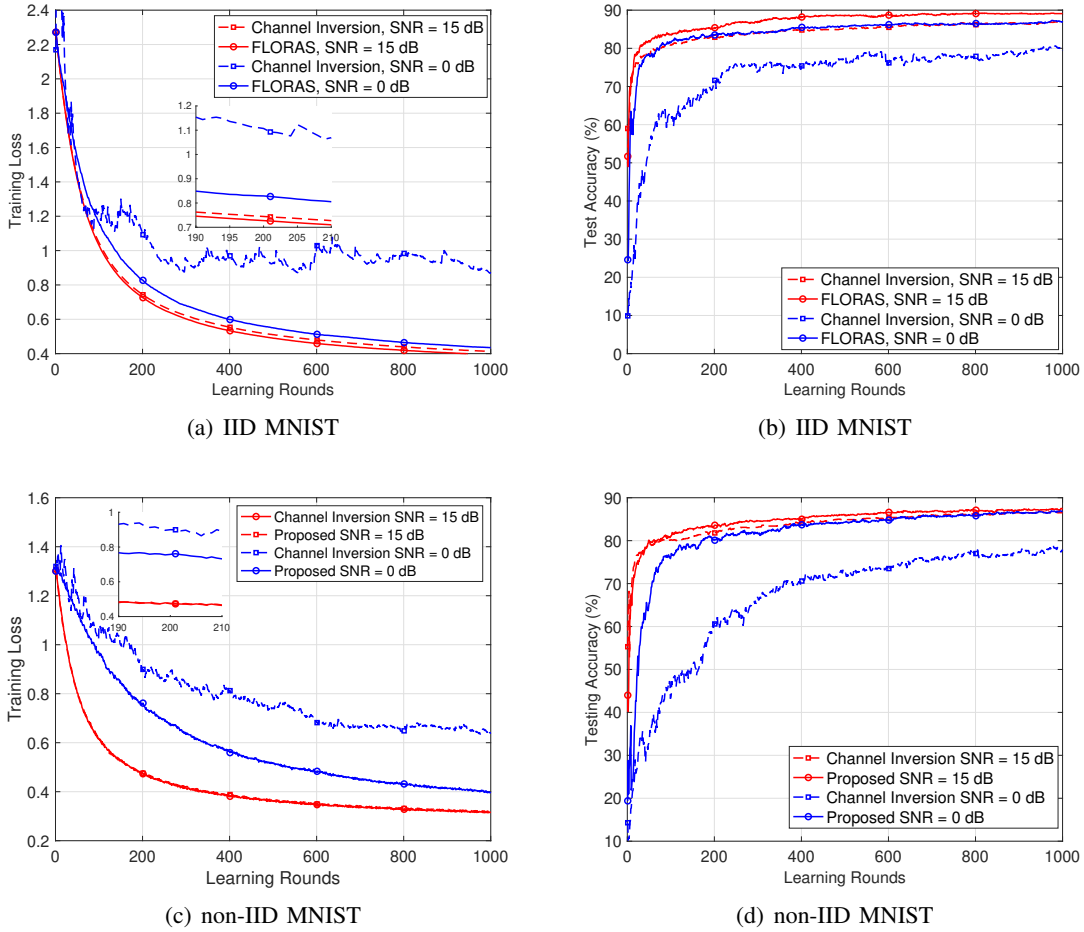


Fig. 4. Training loss/test accuracy versus learning rounds of FLORAS and channel inversion for MNIST dataset under SNR = 0 and 15 dB.

VII. EXPERIMENTS

In this section, we evaluate the performance of FLORAS through numerical experiments. We first compare the learning performance of FLORAS with the widely-investigated channel inversion AirComp method. Then, we evaluate the effect on the convergence rate of various DP levels. In particular, we corroborate the theoretical results via real-world FL tasks on the MNIST dataset. The experiments demonstrate that the proposed method achieves superior performances under various SNRs and other system configurations.

Details on the setup of experiments are as follows. All convergence curves are the average of five independent Monte Carlo trials. The MNIST dataset contains multiple handwritten digit figures of 20×20 pixels. The training set contains 4,000 examples and is evenly distributed over $K = 20$ clients. For the IID case, the data is shuffled and randomly assigned to each client; for the non-IID case, the data is

sorted by labels and each client is then randomly assigned with the data of one label. The test set size is 1,000. We evaluate FLORAS and validate the theoretical results on a multinomial logistic regression task. Specifically, let $f(\mathbf{w}; x_i)$ denote the prediction model with the parameter $\mathbf{w} = (\mathbf{W}, \mathbf{b})$ and the form $f(\mathbf{w}; x_i) = \text{softmax}(\mathbf{W}x_i + \mathbf{b})$. The loss function is given by

$$\text{loss}(\mathbf{w}) = \frac{1}{D} \sum_{i=1}^D \text{CrossEntropy}(f(\mathbf{w}; x_i), \mathbf{y}_i) + \lambda \|\mathbf{w}\|^2.$$

We adopt the regularization parameter $\lambda = 0.01$ in the experiments.

A. Communication Efficiency

We first evaluate the performance of FLORAS compared with the channel inversion method. We assume IID Rayleigh block fading channel $h_k \sim \mathcal{CN}(0, 1)$, $\forall k = 1, \dots, K$. For channel inversion, we adopt a threshold 0.01 for the fading channel gain to avoid deep fading. The following parameters are used for training: local batch size 50, the number of local epochs $E = 1$, and learning rate $\eta = 0.005$ and $\eta = 0.001$ for the IID and non-IID case, respectively.

Fig. 4-(a) and Fig. 4-(b) illustrate the training loss and test accuracy performance versus learning round of FLORAS and channel inversion in high (red line) and low (blue) SNR regimes, respectively. For high SNR (15 dB), FLORAS and channel inversion have similar performance. Although transmitter fading channel cancellation in channel inversion limits the maximum transmission power of each user, its performance does not deteriorate, since noise is not the dominant factor of the convergence. However, we note that, unlike FLORAS, channel inversion requires full CSIT at each client, which not only consumes larger communication overhead, but also increases the dynamic range of the signal, bringing higher hardware cost. The advantages of tFLORAS become conspicuous in the low SNR regime (0 dB), in which noise becomes the dominant factor of the convergence rate. FLORAS allows all participated clients to make full use of transmit power and achieves significantly better performance. As shown in Fig. 4-(b), FLORAS achieves about 7.5% higher test accuracy compared with channel inversion at SNR = 0 dB. This phenomenon becomes more notable in the non-IID dataset as shown in Fig. 4-(c) and Fig. 4-(d), where the performance gap of test accuracy between the proposed method and channel inversion further grows to 10.2%.

B. Differential Privacy

We next evaluate the convergence performance versus different levels of DP. We keep SNR = 20 dB and number of selected user $K = 20$, while changing the size of the orthogonal sequence set \mathcal{A}

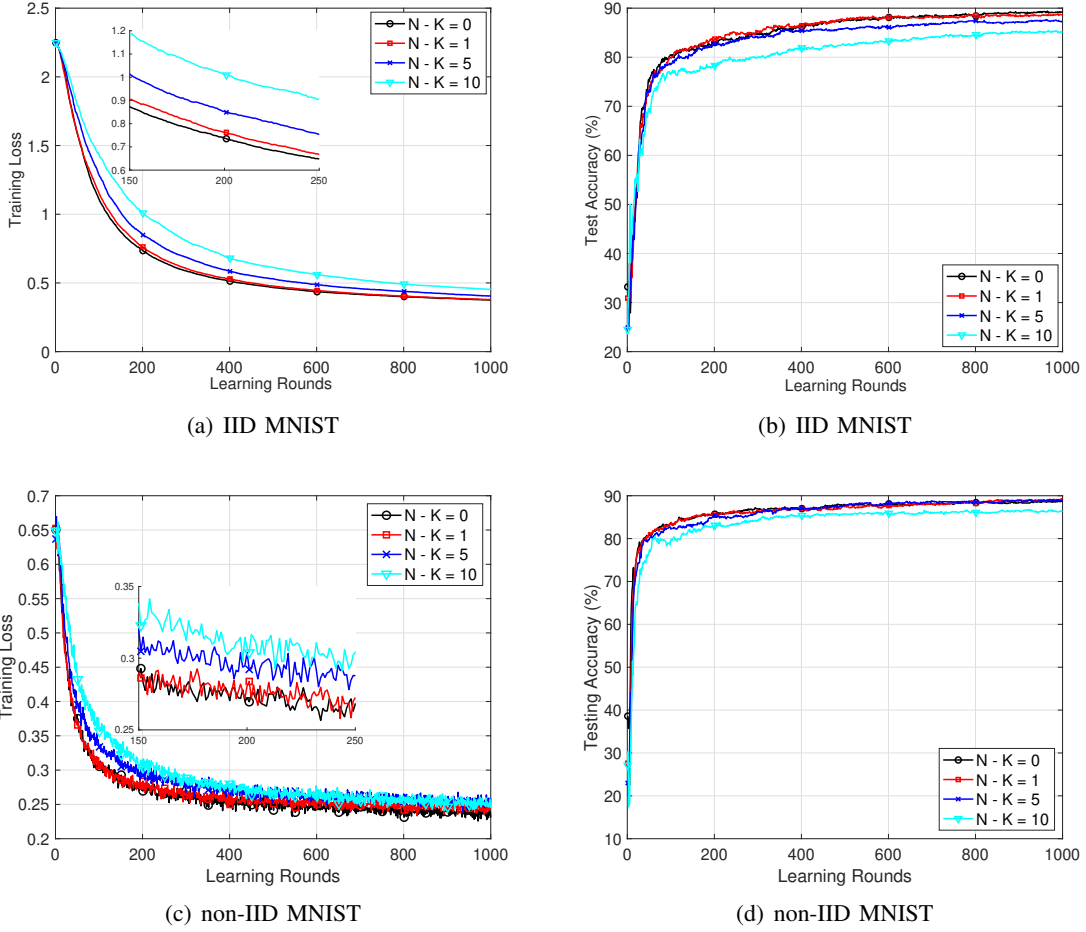


Fig. 5. Training loss/test accuracy versus learning rounds of FLORAS providing different differential privacy levels for MNIST dataset under SNR = 20 dB.

from 20, 21, 25 to 30, i.e., $N - K = 0, 1, 5$ and 10. In each learning round, each user selects its own signature for set \mathcal{A} via the method in Section V-D. As discussed in Section V, the larger size of set \mathcal{A} , the higher DP level FLORAS achieves. The following parameters are used for training: local batch size 20, the number of local epochs $E = 1$, and learning rate $\eta = 0.005$ and $\eta = 0.001$ for IID and non-IID cases, respectively. The training losses with different DP levels are illustrated in Fig. 5-(a) and Fig. 5-(c) of IID and non-IID cases, respectively. It is clear that although a higher privacy level decreases the convergence rate, the machine learning model can still converge with almost the same training loss as the no-differential-privacy case ($N - K = 0$), which is consistent with the theoretical analysis in Section VI. The test accuracies in Fig. 5-(b) and Fig. 5-(d) further validate the effectiveness of FLORAS. We can see that the test accuracies for moderate DP levels ($N - K = 1$ and 5) are almost the same as the case of $N - K = 0$, i.e., we can achieve certain DP levels *almost for free*. Even when $N - K = 10$, the test

accuracy loss is tiny, with about 3.5% and 2.5% compared with the $N - K = 0$ case in the IID and non-IID datasets, respectively.

VIII. CONCLUSION

We have proposed FLORAS, a differentially private AirComp FL framework. Compared with the channel inversion method, FLORAS does not require CSIT and has much more robust performance in the low SNR regime, which is crucial for IoT applications. The flexibility of adjusting the size of the orthogonal sequence set allows us to control both item-level and client-level DP guarantees of the system. From the analyses of convergence and DP of FLORAS, we have established the trade-off between convergence speed and privacy preservation, which has been further validated by experiments on real-world FL tasks.

APPENDIX A

PROOFS OF THEOREMS 1, 2, AND 3

A. Lemmas

We first establish the necessary lemmas for the proofs.

Lemma 2. *Let P and Q be two Cauchy probability distributions $\text{Cauchy}(0, \gamma)$ and $\text{Cauchy}(\theta, \gamma)$, with PDF $P(x) = \frac{1}{\pi} \frac{\gamma}{x^2 + \gamma^2}$ and $Q(x) = \frac{1}{\pi} \frac{\gamma}{(x - \theta)^2 + \gamma^2}$, respectively. $\frac{Q(x)}{P(x)} = \frac{x^2 + \gamma^2}{(x - \theta)^2 + \gamma^2}$ reaches its maximum at $x_{\max} = \theta$ with $\left[\frac{Q(x)}{P(x)}\right]_{\max} = \frac{\theta^2 + \gamma^2}{\gamma^2}$, and its minimum at $x_{\min} = 0$ with $\left[\frac{Q(x)}{P(x)}\right]_{\min} = \frac{\gamma^2}{\theta^2 + \gamma^2}$.*

Proof. The results can be directly obtained by taking the first-order derivative of $\frac{Q(x)}{P(x)}$ and setting $\frac{\partial}{\partial x} \frac{Q(x)}{P(x)} = 0$. \square

Lemma 3 (Proposition 3.3 in [61]). *Let P and Q be probability distributions satisfying $D_{\infty}(P||Q) \leq \epsilon$ and $D_{\infty}(Q||P) \leq \epsilon$. Then $D_{\alpha}(P||Q) \leq \frac{1}{2}\alpha\epsilon^2$ for all $\alpha > 1$.*

Lemma 4 (Proposition 3 in [52]). *If f is an (α, ϵ) -Rényi DP mechanism, it also satisfies $(\epsilon + \frac{\log(1/\delta)}{\alpha - 1}, \delta)$ -DP for any $0 < \delta < 1$.*

B. Proof of Theorem 1

Define neighboring datasets $\mathcal{D} = \bigcup_{i=1}^K \mathcal{D}_i$ and $\mathcal{D}' = \{\bigcup_{i=1, i \neq k}^K \mathcal{D}_i\} \cup \mathcal{D}'_k$, where $\mathcal{D}'_k \triangleq \mathcal{D}_k \cup \{z\}$ has one more element than \mathcal{D}_k . The size of $\{\mathcal{D}_i, i = 1, \dots, K\}$ and \mathcal{D}'_k are D and $D' \triangleq D + 1$, respectively.

Let $d_{\text{batch}} \triangleq |\xi|$ denote the size of the mini batch of SGD for all clients. Hence we have $c = \binom{D}{d_{\text{batch}}}$

and $c' = \binom{D'}{d_{\text{batch}}}$ different mini-batches for dataset $\{\mathcal{D}_i, i = 1, \dots, K\}$ and \mathcal{D}'_k , respectively. We further denote set $\Xi_i \triangleq \{\xi_{i,1}, \dots, \xi_{i,c}\}$ as a collection of all the mini-batches corresponding to $\{\mathcal{D}_i, i = 1, \dots, K\}$. It is straightforward to verify that

$$c' = \binom{D+1}{d_{\text{batch}}} = \binom{D}{d_{\text{batch}}} + \binom{D}{d_{\text{batch}}-1},$$

which reveals that there are $\binom{D}{d_{\text{batch}}}$ mini-batches in \mathcal{D}'_k that are the same as those in Ξ_k , and the remaining $\binom{D}{d_{\text{batch}}-1}$ mini-batches are the ones that contain the data sample z . We denote $\Xi'_k = \{\xi'_{k,1}, \dots, \xi'_{k,c'-c}\}$ as a collection of all the mini-batches that contain the data sample z . Therefore, all the possible mini-batches of \mathcal{D}'_k are in $\Xi_k \cup \Xi'_k$.

We note that, for K clients, there are total c^K combinations of mini-batches in \mathcal{D} , which we denote as $\xi_j \triangleq \{\xi_{1,c_1}, \dots, \xi_{i,c_i}, \dots, \xi_{K,c_K}\}, j = 1, \dots, c^K$, where $\xi_{i,c_i} \in \Xi_i, \forall i = 1, \dots, K$. As for \mathcal{D}' , there are total $c'c^{K-1}$ mini-batch combinations. Besides the same c^K combinations in \mathcal{D} , there are additional $(c' - c)c^{K-1}$ mini-batch combinations in \mathcal{D}' , among which the mini-batch of the k -th client is chosen from Ξ'_k . We denote them similarly as $\xi'_j \triangleq \{\xi_{1,c_1}, \dots, \xi'_{i,c'_i}, \dots, \xi_{K,c_K}\}, j = 1, \dots, (c' - c)c^{K-1}$, where $\xi_{i,c_i} \in \Xi_i, \forall i \neq k$, and $\xi'_{k,c'_i} \in \Xi'_k$. In addition, we use $g(\xi_j)$ to denote the noise-free global models calculated from mini-batch combination ξ_j . Building on this, the mechanism $\mathcal{M}(\mathcal{D})$ can be viewed as a random vector sampling from the following distribution:

$$\mathcal{M}(\mathcal{D}) = \sum_{j=1}^{c^K} \frac{1}{c^K} \text{Cauchy}(g(\xi_j), (N - K)\mathbf{I}_d).$$

Similarly,

$$\begin{aligned} \mathcal{M}(\mathcal{D}') &= \sum_{j=1}^{c^K} \frac{1}{c^{K-1}c'} \text{Cauchy}(g(\xi_j), (N - K)\mathbf{I}_d) \\ &+ \sum_{j=1}^{(c'-c)c^{K-1}} \frac{1}{c^{K-1}c'} \text{Cauchy}(g(\xi'_j), (N - K)\mathbf{I}_d). \end{aligned}$$

For mathematical simplicity, we assume $\text{mod}(D_k + 1, d_{\text{batch}}) = 0$. Based on the fact that

$$\frac{c}{c'} = \frac{\binom{D_k}{d_{\text{batch}}}}{\binom{D_k + 1}{d_{\text{batch}}}} = 1 - \frac{d_{\text{batch}}}{D_k + 1},$$

$\mathcal{M}(\mathcal{D}')$ can be re-written as

$$\begin{aligned} \mathcal{M}(\mathcal{D}') &= \frac{1}{c^{K-1}c'} \sum_{j=1}^{c^K} \left[\text{Cauchy}(g(\boldsymbol{\xi}_j), (N-K)\mathbf{I}_d) \right. \\ &\quad \left. + \frac{c' - c}{c} \text{Cauchy}(g(\boldsymbol{\xi}'_{\lceil j * \frac{c' - c}{c} \rceil}), (N-K)\mathbf{I}_d) \right] \\ &= \frac{1}{c^K} \sum_{j=1}^{c^K} \left[\frac{c}{c'} \text{Cauchy}(g(\boldsymbol{\xi}_j), (N-K)\mathbf{I}_d) \right. \\ &\quad \left. + \frac{c}{c'} \frac{c' - c}{c} \text{Cauchy}(g(\boldsymbol{\xi}'_{\lceil j * \frac{c' - c}{c} \rceil}), (N-K)\mathbf{I}_d) \right] \\ &= \sum_{j=1}^{c^K} \frac{1}{c^K} \left[\left(1 - \frac{d_{\text{batch}}}{D_k + 1} \right) \text{Cauchy}(g(\boldsymbol{\xi}_j), (N-K)\mathbf{I}_d) \right. \\ &\quad \left. + \frac{d_{\text{batch}}}{D_k + 1} \text{Cauchy}(\boldsymbol{\xi}'_{\lceil j * \frac{c' - c}{c} \rceil}, (N-K)\mathbf{I}_d) \right] \end{aligned}$$

where the first equality comes from breaking the original summation of $(c' - c)c^{K-1}$ items into c^K groups (each of size $\frac{c' - c}{c}$). We next bound the Rényi divergence for $\alpha = +\infty$. Define $\gamma = N - K$ and $q = \frac{d_{\text{batch}}}{D_k + 1}$. Since Rényi divergence is quasi-convex, we have

$$\begin{aligned} D_\infty(\mathcal{M}(\mathcal{D}) || \mathcal{M}(\mathcal{D}')) &\leq \sup_j D_\infty \left[\text{Cauchy}(g(\boldsymbol{\xi}_j), \gamma \mathbf{I}_d) || (1 - q) \text{Cauchy}(g(\boldsymbol{\xi}_j), \gamma \mathbf{I}_d) \right. \\ &\quad \left. + q \text{Cauchy}(g(\boldsymbol{\xi}'_{\lceil j * \frac{c' - c}{c} \rceil}), \gamma \mathbf{I}_d) \right] \\ &\leq \sup_j D_\infty \left[\text{Cauchy}(0, \gamma \mathbf{I}_d) || (1 - q) \text{Cauchy}(0, \gamma \mathbf{I}_d) \right. \\ &\quad \left. + q \text{Cauchy}(g(\boldsymbol{\xi}'_{\lceil j * \frac{c' - c}{c} \rceil}) - g(\boldsymbol{\xi}_j), \gamma \mathbf{I}_d) \right]. \end{aligned}$$

As shown in (6), $\left\| g(\boldsymbol{\xi}'_{\lceil j * \frac{c' - c}{c} \rceil}) - g(\boldsymbol{\xi}_j) \right\|_2 \leq 2C$. Therefore, via a rotation, we have that $g(\boldsymbol{\xi}'_{\lceil j * \frac{c' - c}{c} \rceil}) - g(\boldsymbol{\xi}_j) = c_\xi \mathbf{e}_1$ where $c_\xi \leq 2C$. By the additivity of Rényi divergence for product distributions [62], we

have that

$$\begin{aligned} & D_{\infty}(\mathcal{M}(\mathcal{D})||\mathcal{M}(\mathcal{D}')) \\ & \leq D_{\infty}[\text{Cauchy}(0, \gamma)|| (1-q)\text{Cauchy}(0, \gamma) + q\text{Cauchy}(2C, \gamma)]. \end{aligned}$$

We next bound $D_{\infty}(\mathcal{M}(\mathcal{D})||\mathcal{M}(\mathcal{D}'))$ and $D_{\infty}(\mathcal{M}(\mathcal{D}')||\mathcal{M}(\mathcal{D}))$. Based on the results in Lemma 2, we have

$$\max \left[\frac{\text{Cauchy}(2C, \gamma)}{\text{Cauchy}(0, \gamma)} \right] = \frac{4C^2 + \gamma^2}{\gamma^2},$$

and

$$\min \left[\frac{\text{Cauchy}(2C, \gamma)}{\text{Cauchy}(0, \gamma)} \right] = \frac{\gamma^2}{4C^2 + \gamma^2}.$$

Therefore, $D_{\infty}(\mathcal{M}(\mathcal{D})||\mathcal{M}(\mathcal{D}'))$ and $D_{\infty}(\mathcal{M}(\mathcal{D}')||\mathcal{M}(\mathcal{D}))$ can be bounded as follows, respectively:

$$\begin{aligned} & D_{\infty}[(1-q)\text{Cauchy}(0, \gamma) + q\text{Cauchy}(2C, \gamma)||\text{Cauchy}(0, \gamma)] \\ & = \sup \log \left[1 - q + q \frac{\text{Cauchy}(2C, \gamma)}{\text{Cauchy}(0, \gamma)} \right] \leq \log \left(1 + \frac{4qC^2}{\gamma^2} \right) \end{aligned}$$

and

$$\begin{aligned} & D_{\infty}[\text{Cauchy}(0, \gamma)|| (1-q)\text{Cauchy}(0, \gamma) + q\text{Cauchy}(2C, \gamma)] \\ & = \sup \log \left[\frac{1}{1 - q + q \frac{\text{Cauchy}(2C, \gamma)}{\text{Cauchy}(0, \gamma)}} \right] \leq \log \left(1 + \frac{4qC^2}{(1-q)4C^2 + \gamma^2} \right). \end{aligned}$$

It is straightforward to verify that $\frac{4qC^2}{\gamma^2} \geq \frac{4qC^2}{(1-q)4C^2 + \gamma^2}, \forall 0 < q < 1$. Therefore, $D_{\infty}(\mathcal{M}(\mathcal{D})||\mathcal{M}(\mathcal{D}'))$ and $D_{\infty}(\mathcal{M}(\mathcal{D}')||\mathcal{M}(\mathcal{D}))$ are both bounded by $\log \left(1 + \frac{4qC^2}{\gamma^2} \right)$. Based on Lemma 3, we can guarantee $D_{\alpha}(\mathcal{M}(\mathcal{D})||\mathcal{M}(\mathcal{D}')) \leq \frac{1}{2}\alpha \log^2 \left(1 + \frac{4qC^2}{\gamma^2} \right)$, which completes the proof.

C. Proof of Theorem 2

Based on Theorem 1 and the composition rule of Rényi DP as shown in Lemma 4, the Rényi DP guarantee for total T learning rounds is $\left[\frac{1}{2}T\alpha \log^2 \left(1 + \frac{4qC^2}{\gamma^2} \right), \alpha \right]$ -Rényi DP. Therefore, the proposed design satisfies (ϵ', δ) -DP, where

$$\begin{aligned} \epsilon' &= \min_{\alpha > 1} \frac{1}{2}T\alpha \log^2 \left(1 + \frac{4qC^2}{(N-K)^2} \right) + \frac{\log(1/\delta)}{\alpha - 1} \\ &\geq \sqrt{2T \log(1/\delta)} \log \left(1 + \frac{4qC^2}{(N-K)^2} \right) \\ &\quad + \frac{1}{2}T \log^2 \left(1 + \frac{4qC^2}{(N-K)^2} \right). \end{aligned}$$

D. Proof of Theorem 3

Define neighboring datasets $\mathcal{D} = \bigcup_{i=1}^K \mathcal{D}_i$ and $\mathcal{D}' = \{\bigcup_{i=1, i \neq k}^M \mathcal{D}_i\} \cup \mathcal{D}'_k$, where \mathcal{D}'_k can be entirely different from the local dataset of client k . Therefore, the mechanism $\mathcal{M}(\mathcal{D})$ samples from a Cauchy distribution with central $g(\mathcal{D})$, i.e.,

$$\mathcal{M}(\mathcal{D}) = \text{Cauchy}(g(\mathcal{D}), (N - K)\mathbf{I}_d).$$

Similarly,

$$\mathcal{M}(\mathcal{D}') = \text{Cauchy}(g(\mathcal{D}'), (N - K)\mathbf{I}_d).$$

By the definition of $\gamma \triangleq N - K$, we have

$$\begin{aligned} D_\infty(\mathcal{M}(\mathcal{D}) || \mathcal{M}(\mathcal{D}')) &= D_\infty[\text{Cauchy}(g(\mathcal{D}), \gamma\mathbf{I}_d) || \text{Cauchy}(g(\mathcal{D}'), \gamma\mathbf{I}_d)] \\ &= D_\infty[\text{Cauchy}(0, \gamma\mathbf{I}_d) || \text{Cauchy}(g(\mathcal{D}') - g(\mathcal{D}), \gamma\mathbf{I}_d)]. \end{aligned}$$

Since $\|g(\mathcal{D}') - g(\mathcal{D})\|_2 \leq 2C$, by applying a rotation, we have that $g(\mathcal{D}') - g(\mathcal{D}) = c_\xi \mathbf{e}_1$ where $c_\xi \leq 2C$.

By the additivity of Rényi divergence for product distributions [62], we have that

$$D_\infty(\mathcal{M}(\mathcal{D}) || \mathcal{M}(\mathcal{D}')) \leq D_\infty[\text{Cauchy}(0, \gamma) || \text{Cauchy}(2C, \gamma)].$$

Based on Lemma 2 and following the similar techniques in Appendix A-B, $D_\infty(\mathcal{M}(\mathcal{D}_k) || \mathcal{M}(\mathcal{D}'_k))$ and $D_\infty(\mathcal{M}(\mathcal{D}'_k) || \mathcal{M}(\mathcal{D}_k))$ can both be bounded by $\log\left(1 + \frac{4C^2}{\gamma^2}\right)$. Again, based on Lemma 3, we can guarantee $D_\alpha(\mathcal{M}(\mathcal{D}) || \mathcal{M}(\mathcal{D}')) \leq \frac{1}{2}\alpha \log^2\left(1 + \frac{4C^2}{\gamma^2}\right)$, which completes the single round DP guarantee. The proof of the client-level DP guarantee for the composition of T rounds follows the same as that in Appendix A-C.

APPENDIX B

PROOF OF THEOREM 4

With a slight abuse of notation, we change the timeline to be with respect to the overall SGD iteration time steps instead of the communication rounds, i.e.,

$$t = \underbrace{1, \dots, E}_{\text{round 1}}, \underbrace{E+1, \dots, 2E}_{\text{round 2}}, \dots, \dots, \underbrace{(T-1)E+1, \dots, TE}_{\text{round } T}.$$

Note that the global model \mathbf{w}_t is only accessible at the clients for specific $t \in \mathcal{I}_E$, where $\mathcal{I}_E = \{nE \mid n = 1, 2, \dots\}$, i.e., the time steps for communication. The notations for η_t are similarly adjusted to this extended timeline, but their values remain constant inside the same round. The key technique in the proof is the *perturbed iterate framework* in [63]. In particular, we first define the following variables for client $k \in [M]$:

$$\begin{aligned} \mathbf{v}_{t+1}^k &\triangleq \mathbf{w}_t^k - \eta_t \nabla \tilde{f}_k(\mathbf{w}_t^k); \\ \mathbf{u}_{t+1}^k &\triangleq \begin{cases} \mathbf{v}_{t+1}^k & \text{if } t+1 \notin \mathcal{I}_E, \\ \frac{1}{K} \sum_{k=1}^K \mathbf{v}_{t+1}^k & \text{if } t+1 \in \mathcal{I}_E; \end{cases} \\ \mathbf{w}_{t+1}^k &\triangleq \begin{cases} \mathbf{v}_{t+1}^k & \text{if } t+1 \notin \mathcal{I}_E, \\ \mathbf{u}_{t+1}^k + \frac{1}{K} \mathbf{n}_{t+1} & \text{if } t+1 \in \mathcal{I}_E; \end{cases} \end{aligned}$$

where

$$\mathbf{n}_{t+1} \triangleq \left[\sum_{k=K+1}^N \frac{\mathbf{a}_k^T \mathbf{n}_1}{\mathbf{a}_k^T \mathbf{n}_s}, \dots, \sum_{k=K+1}^N \frac{\mathbf{a}_k^T \mathbf{n}_d}{\mathbf{a}_k^T \mathbf{n}_s} \right]^T \in \mathbb{C}^{d \times 1}.$$

Then, we construct the following *virtual sequences*:

$$\bar{\mathbf{v}}_t = \frac{1}{M} \sum_{k=1}^M \mathbf{v}_t^k, \quad \bar{\mathbf{u}}_t = \frac{1}{M} \sum_{k=1}^M \mathbf{u}_t^k, \quad \text{and} \quad \bar{\mathbf{w}}_t = \frac{1}{M} \sum_{k=1}^M \mathbf{w}_t^k.$$

We also define $\bar{\mathbf{g}}_t = \frac{1}{M} \sum_{k=1}^M \nabla f_k(\mathbf{w}_t^k)$ and $\mathbf{g}_t = \frac{1}{M} \sum_{k=1}^M \nabla \tilde{f}_k(\mathbf{w}_t^k)$ for convenience. Therefore, $\bar{\mathbf{v}}_{t+1} = \bar{\mathbf{w}}_t - \eta_t \mathbf{g}_t$ and $\mathbb{E}[\mathbf{g}_t] = \bar{\mathbf{g}}_t$. Note that the global model \mathbf{w}_{t+1} is only meaningful when $t+1 \in \mathcal{I}_E$. Hence, we have

$$\mathbf{w}_{t+1} = \frac{1}{K} \sum_{k=1}^K \mathbf{w}_{t+1}^k = \mathbf{w}_{t+1}^k = \frac{1}{M} \sum_{k=1}^M \mathbf{w}_{t+1}^k = \bar{\mathbf{w}}_{t+1}.$$

Thus it is sufficient to analyze the convergence of $\|\bar{\mathbf{w}}_{t+1} - \mathbf{w}^*\|^2$ to evaluate FLORAS.

A. Lemmas

Lemma 5. *Let Assumptions 1-4 hold, η_t is non-increasing, and $\eta_t \leq 2\eta_{t+E}$ for all $t \geq 0$. If $\eta_t \leq 1/(4L)$, we have*

$$\begin{aligned} \mathbb{E} \|\bar{\mathbf{v}}_{t+1} - \mathbf{w}^*\|^2 &\leq (1 - \eta_t \mu) \mathbb{E} \|\bar{\mathbf{w}}_t - \mathbf{w}^*\|^2 \\ &+ \eta_t^2 \left(\sum_{k=1}^M H_k^2 / M^2 + 6L\Gamma + 8(E-1)^2 H^2 \right) \end{aligned}$$

Lemma 5 establishes a bound for the one-step SGD. This result only concerns the local model update and is not impacted by the noisy communication. The derivation is similar to the technique in [59].

Lemma 6. *Let Assumptions 1-4 hold. With $\eta_t \leq 2\eta_{t+E}$ for all $t \geq 0$ and $\forall t+1 \in \mathcal{I}_E$, we have*

$$\mathbb{E}[\bar{\mathbf{u}}_{t+1}] = \bar{\mathbf{v}}_{t+1}, \mathbb{E}\|\bar{\mathbf{v}}_{t+1} - \bar{\mathbf{u}}_{t+1}\|^2 \leq \frac{M-K}{M-1} \frac{4}{K} \eta_t^2 E^2 H^2.$$

Lemma 6 demonstrates a bound for the uniformly random selection. This result bounded the extra “noise” brought by *partial participation*. We note that $\mathbb{E}\|\bar{\mathbf{v}}_{t+1} - \bar{\mathbf{u}}_{t+1}\|^2 = 0$ in the full participation case, where $K = M$. The derivation is similar to the technique in [59].

Lemma 7. *Let Assumptions 1-4 hold. With $\eta_t \leq 2\eta_{t+E}$ for all $t \geq 0$ and $\forall t+1 \in \mathcal{I}_E$, we have $\mathbb{E}[\bar{\mathbf{w}}_{t+1}] = \bar{\mathbf{u}}_{t+1}$ and*

$$\begin{aligned} \mathbb{E}\|\bar{\mathbf{w}}_{t+1} - \bar{\mathbf{u}}_{t+1}\|^2 &\leq \frac{64C^2}{K^2\epsilon^2 \arctan\left(\frac{B\epsilon}{4C}\right)} \\ &\quad \times \left[\frac{B\epsilon}{4C} - \arctan\left(\frac{B\epsilon}{4C}\right) \right] \eta_t^2 E^2 H^2. \end{aligned}$$

Proof. Since \mathbf{n}_{t+1} is a truncated Cauchy random vector with each element truncated in the interval $[-B, B]$, we have $\mathbb{E}[\mathbf{n}_{t+1}] = \mathbf{0}$ and

$$\begin{aligned} \mathbb{E}[\mathbf{n}_{t+1}^H \mathbf{n}_{t+1}] &= \frac{d(N-K)^2}{\arctan\left(\frac{B}{N-K}\right)} \left[\frac{B}{N-K} - \arctan\left(\frac{B}{N-K}\right) \right] \\ &= \frac{16dC^2}{\epsilon^2 \arctan\left(\frac{B\epsilon}{4C}\right)} \left[\frac{B\epsilon}{4C} - \arctan\left(\frac{B\epsilon}{4C}\right) \right], \end{aligned}$$

by utilizing the results in [64]. By taking the expectation over the randomness of truncated Cauchy noise, we have

$$\mathbb{E}[\bar{\mathbf{w}}_{t+1}] = \mathbb{E}\left[\frac{1}{M} \sum_{k=1}^M \mathbf{w}_{t+1}^k \right] = \mathbb{E}[\mathbf{w}_{t+1}^k] = \bar{\mathbf{u}}_{t+1}.$$

We next evaluate the variance of $\bar{\mathbf{w}}_{t+1}$,

$$\begin{aligned} \mathbb{E}\|\bar{\mathbf{w}}_{t+1} - \bar{\mathbf{u}}_{t+1}\|^2 &= \mathbb{E}\left\| \frac{1}{K} \mathbf{n}_{t+1} \right\|^2 \\ &= \frac{16dC^2}{K^2\epsilon^2 \arctan\left(\frac{B\epsilon}{4C}\right)} \left[\frac{B\epsilon}{4C} - \arctan\left(\frac{B\epsilon}{4C}\right) \right] \\ &= \frac{16C^2}{K^3\epsilon^2 \arctan\left(\frac{B\epsilon}{4C}\right)} \left[\frac{B\epsilon}{4C} - \arctan\left(\frac{B\epsilon}{4C}\right) \right] \sum_{k=1}^K \mathbb{E}\|\mathbf{x}_t^k\|^2 \end{aligned}$$

$$\begin{aligned}
&\leq \frac{16}{K^3 \epsilon^2 \arctan\left(\frac{B\epsilon}{4C}\right)} \left[\frac{B\epsilon}{4C} - \arctan\left(\frac{B\epsilon}{4C}\right) \right] \\
&\quad \times \sum_{k=1}^K E \sum_{i=t+1-E}^t \mathbb{E} \left\| \eta_i \nabla \tilde{f}_k(\mathbf{w}_i^k) \right\|^2 \\
&\leq \frac{16}{K^2 \epsilon^2 \arctan\left(\frac{B\epsilon}{4C}\right)} \left[\frac{B\epsilon}{4C} - \arctan\left(\frac{B\epsilon}{4C}\right) \right] \eta_{t+1-E}^2 E^2 H^2 \\
&\leq \frac{64}{K^2 \epsilon^2 \arctan\left(\frac{B\epsilon}{4C}\right)} \left[\frac{B\epsilon}{4C} - \arctan\left(\frac{B\epsilon}{4C}\right) \right] \eta_t^2 E^2 H^2,
\end{aligned}$$

where in the last inequality we use the fact that η_t is non-increasing and $\eta_{t+1-E} \leq 2\eta_t$. \square

B. Proof of Theorem 4

We next consider the convergence of $\mathbb{E} \|\bar{\mathbf{w}}_{t+1} - \mathbf{w}^*\|^2$.

1) If $t+1 \notin \mathcal{I}_E$, $\bar{\mathbf{v}}_{t+1} = \bar{\mathbf{w}}_{t+1}$. Using Lemma 5, we have:

$$\begin{aligned}
\mathbb{E} \|\bar{\mathbf{w}}_{t+1} - \mathbf{w}^*\|^2 &= \mathbb{E} \|\bar{\mathbf{v}}_{t+1} - \mathbf{w}^*\|^2 \leq (1 - \eta_t \mu) \mathbb{E} \|\bar{\mathbf{w}}_t - \mathbf{w}^*\|^2 \\
&\quad + \eta_t^2 \left[\sum_{k=1}^M \frac{H_k^2}{M^2} + 6L\Gamma + 8(E-1)^2 H^2 \right].
\end{aligned}$$

2) If $t+1 \in \mathcal{I}_E$, to evaluate the convergence of $\mathbb{E} \|\bar{\mathbf{w}}_{t+1} - \mathbf{w}^*\|^2$, we establish

$$\begin{aligned}
\|\bar{\mathbf{w}}_{t+1} - \mathbf{w}^*\|^2 &= \|\bar{\mathbf{w}}_{t+1} - \bar{\mathbf{u}}_{t+1} + \bar{\mathbf{u}}_{t+1} - \mathbf{w}^*\|^2 \\
&= \underbrace{\|\bar{\mathbf{w}}_{t+1} - \bar{\mathbf{u}}_{t+1}\|^2}_{A_1} + \underbrace{\|\bar{\mathbf{u}}_{t+1} - \mathbf{w}^*\|^2}_{A_2} + \underbrace{2 \langle \bar{\mathbf{w}}_{t+1} - \bar{\mathbf{u}}_{t+1}, \bar{\mathbf{u}}_{t+1} - \mathbf{w}^* \rangle}_{A_3}.
\end{aligned}$$

We first note that the expectation of A_3 over the noise distribution is zero since we have $\mathbb{E} [\bar{\mathbf{u}}_{t+1} - \bar{\mathbf{w}}_{t+1}] = \mathbf{0}$ and the expectation of A_1 can be bounded using Lemma 7. We write A_2 as

$$\begin{aligned}
\|\bar{\mathbf{u}}_{t+1} - \mathbf{w}^*\|^2 &= \|\bar{\mathbf{u}}_{t+1} - \bar{\mathbf{v}}_{t+1} + \bar{\mathbf{v}}_{t+1} - \mathbf{w}^*\|^2 \\
&= \underbrace{\|\bar{\mathbf{u}}_{t+1} - \bar{\mathbf{v}}_{t+1}\|^2}_{B_1} + \underbrace{\|\bar{\mathbf{v}}_{t+1} - \mathbf{w}^*\|^2}_{B_2} + \underbrace{2 \langle \bar{\mathbf{u}}_{t+1} - \bar{\mathbf{v}}_{t+1}, \bar{\mathbf{v}}_{t+1} - \mathbf{w}^* \rangle}_{B_3}.
\end{aligned}$$

Similarly, the expectation of B_3 over the noise distribution is zero since we have $\mathbb{E} [\bar{\mathbf{u}}_{t+1} - \bar{\mathbf{v}}_{t+1}] = \mathbf{0}$ and the expectation of B_1 can be bounded using Lemma 6. Therefore, we have

$$\begin{aligned}
\mathbb{E} \|\bar{\mathbf{w}}_{t+1} - \mathbf{w}^*\|^2 &\leq \mathbb{E} \|\bar{\mathbf{v}}_{t+1} - \mathbf{w}^*\|^2 + \frac{M-K}{M-1} \frac{4}{K} \eta_t^2 E^2 H^2 \\
&\quad + \frac{64C^2}{K^2 \epsilon^2 \arctan\left(\frac{B\epsilon}{4C}\right)} \left[\frac{B\epsilon}{4C} - \arctan\left(\frac{B\epsilon}{4C}\right) \right] \eta_t^2 E^2 H^2 \\
&\leq (1 - \eta_t \mu) \mathbb{E} \|\bar{\mathbf{w}}_t - \mathbf{w}^*\|^2 + \eta_t^2 \left[\sum_{k=1}^M \frac{H_k^2}{M^2} + 6L\Gamma \right]
\end{aligned}$$

$$\begin{aligned}
& +8(E-1)^2H^2 + \frac{M-K}{M-1} \frac{4}{K} \eta_t^2 E^2 H^2 + \frac{64C^2}{K^2 \epsilon^2 \arctan\left(\frac{B\epsilon}{4C}\right)} \\
& \times \left[\frac{B\epsilon}{4C} - \arctan\left(\frac{B\epsilon}{4C}\right) \right] E^2 H^2 \Big].
\end{aligned}$$

Let $\Delta_t = \mathbb{E} \|\bar{\mathbf{w}}_t - \mathbf{w}^*\|^2$. No matter whether $t+1 \in \mathcal{I}_E$ or $t+1 \notin \mathcal{I}_E$, we always have

$$\Delta_{t+1} \leq (1 - \eta_t \mu) \Delta_t + \eta_t^2 G$$

where

$$\begin{aligned}
G = & \left[\sum_{k=1}^M \frac{H_k^2}{M^2} + 6L\Gamma + 8(E-1)^2H^2 + \frac{M-K}{M-1} \frac{4}{K} \eta_t^2 E^2 H^2 \right. \\
& \left. + \frac{64}{K^2 \epsilon^2 \arctan\left(\frac{B\epsilon}{4C}\right)} \left[\frac{B\epsilon}{4C} - \arctan\left(\frac{B\epsilon}{4C}\right) \right] E^2 H^2 \right].
\end{aligned}$$

Define $v \triangleq \max\{\frac{4G}{\mu^2}, (1+\gamma)\Delta_1\}$, by choosing $\eta_t = \frac{2}{\mu(t+\gamma)}$, we can prove $\Delta_t \leq \frac{v}{t+\gamma}$ by induction:

$$\begin{aligned}
\Delta_{t+1} & \leq \left(1 - \frac{2}{t+\gamma}\right) \Delta_t + \frac{4G}{\mu^2(t+\gamma)^2} \\
& = \frac{t+\gamma-2}{(t+\gamma)^2} v + \frac{4G}{\mu^2(t+\gamma)^2} \\
& = \frac{t+\gamma-1}{(t+\gamma)^2} v + \left(\frac{4G}{\mu^2(t+\gamma)^2} - \frac{v}{(t+\gamma)^2} \right) \\
& \leq \frac{v}{t+\gamma+1}.
\end{aligned}$$

By the L -smoothness of f and $v \leq \frac{4G}{\mu^2} + (1+\gamma)\Delta_1$, we prove Theorem 4.

REFERENCES

- [1] X. Wei, T. Wang, R. Huang, C. Shen, J. Yang, and H. V. Poor, “FLORAS: Differentially private wireless federated learning using orthogonal sequences,” in *Proc. IEEE Int. Conf. Commun.*, May 2023, pp. 1–6.
- [2] B. McMahan, E. Moore, D. Ramage, S. Hampson, and B. A. y Arcas, “Communication-efficient learning of deep networks from decentralized data,” in *Proc. Artificial Intelligence and Statistics*, Fort Lauderdale, FL, USA, Apr. 2017, pp. 1273–1282.
- [3] J. Konecny, H. B. McMahan, F. X. Yu, P. Richtarik, A. T. Suresh, and D. Bacon, “Federated learning: Strategies for improving communication efficiency,” in *Proc. NIPS Workshop on Private Multi-Party Machine Learning*, 2016.
- [4] B. McMahan, E. Moore, D. Ramage, S. Hampson, and B. A. y Arcas, “Communication-efficient learning of deep networks from decentralized data,” in *Artificial intelligence and statistics*. PMLR, 2017, pp. 1273–1282.
- [5] S. Niknam, H. S. Dhillon, and J. H. Reed, “Federated learning for wireless communications: Motivation, opportunities, and challenges,” *IEEE Commun. Mag.*, vol. 58, no. 6, pp. 46–51, 2020.
- [6] G. Zhu, Y. Wang, and K. Huang, “Broadband analog aggregation for low-latency federated edge learning,” *IEEE Trans. Wireless Commun.*, vol. 19, no. 1, pp. 491–506, 2020.

- [7] D. Tse and P. Viswanath, *Fundamentals of Wireless Communication*. Cambridge University Press, 2005.
- [8] G. Zhu, J. Xu, K. Huang, and S. Cui, "Over-the-air computing for wireless data aggregation in massive IoT," *IEEE Wireless Commun.*, vol. 28, no. 4, pp. 57–65, 2021.
- [9] R. Shokri and V. Shmatikov, "Privacy-preserving deep learning," in *Proc. 22nd ACM SIGSAC Conference on Computer and Communications Security*, 2015, pp. 1310–1321.
- [10] Z. Wang, M. Song, Z. Zhang, Y. Song, Q. Wang, and H. Qi, "Beyond inferring class representatives: User-level privacy leakage from federated learning," in *IEEE Int. Conf. Comput. Commun.*, 2019, pp. 2512–2520.
- [11] C. Ma, J. Li, M. Ding, H. H. Yang, F. Shu, T. Q. Quek, and H. V. Poor, "On safeguarding privacy and security in the framework of federated learning," *IEEE Network*, vol. 34, no. 4, pp. 242–248, 2020.
- [12] C. Dwork, A. Roth *et al.*, "The algorithmic foundations of differential privacy," *Foundations and Trends® in Theoretical Computer Science*, vol. 9, no. 3–4, pp. 211–407, 2014.
- [13] D. Levy, Z. Sun, K. Amin, S. Kale, A. Kulesza, M. Mohri, and A. T. Suresh, "Learning with user-level privacy," *Advances in Neural Information Systems*, vol. 34, pp. 12 466–12 479, 2021.
- [14] B. Nazer and M. Gastpar, "Computation over multiple-access channels," *IEEE Trans. Inf. Theory*, vol. 53, no. 10, pp. 3498–3516, 2007.
- [15] K. Yang, T. Jiang, Y. Shi, and Z. Ding, "Federated learning via over-the-air computation," *IEEE Trans. Wireless Commun.*, vol. 19, no. 3, pp. 2022–2035, 2020.
- [16] M. M. Amiri and D. Gündüz, "Federated learning over wireless fading channels," *IEEE Trans. Wireless Commun.*, vol. 19, no. 5, pp. 3546–3557, 2020.
- [17] X. Cao, G. Zhu, J. Xu, and K. Huang, "Optimal power control for over-the-air computation," in *Proc. 2019 IEEE Global Communications Conference (GLOBECOM)*, 2019, pp. 1–6.
- [18] M. Chen, H. V. Poor, W. Saad, and S. Cui, "Convergence time optimization for federated learning over wireless networks," *IEEE Trans. Wireless Commun.*, vol. 20, no. 4, pp. 2457–2471, 2020.
- [19] J. Xu and H. Wang, "Client selection and bandwidth allocation in wireless federated learning networks: A long-term perspective," *IEEE Trans. Wireless Commun.*, vol. 20, no. 2, pp. 1188–1200, 2021.
- [20] Y. Sun, S. Zhou, Z. Niu, and D. Gündüz, "Dynamic scheduling for over-the-air federated edge learning with energy constraints," *IEEE J. Select. Areas Commun.*, vol. 40, no. 1, pp. 227–242, 2021.
- [21] X. Ma, H. Sun, Q. Wang, and R. Q. Hu, "User scheduling for federated learning through over-the-air computation," in *Proc. IEEE 94th Vehicular Technology Conference (VTC2021-Fall)*, 2021, pp. 1–5.
- [22] H.-S. Lee and J.-W. Lee, "Adaptive transmission scheduling in wireless networks for asynchronous federated learning," *IEEE J. Select. Areas Commun.*, vol. 39, no. 12, pp. 3673–3687, 2021.
- [23] M. M. Wadu, S. Samarakoon, and M. Bennis, "Joint client scheduling and resource allocation under channel uncertainty in federated learning," *IEEE Trans. Commun.*, vol. 69, no. 9, pp. 5962–5974, 2021.
- [24] T. Sery and K. Cohen, "On analog gradient descent learning over multiple access fading channels," *IEEE Trans. Signal Processing*, vol. 68, pp. 2897–2911, 2020.
- [25] Z. Lin, X. Li, V. K. Lau, Y. Gong, and K. Huang, "Deploying federated learning in large-scale cellular networks: Spatial convergence analysis," *IEEE Trans. Wireless Commun.*, vol. 21, no. 3, pp. 1542–1556, 2021.
- [26] O. Aygün, M. Kazemi, D. Gündüz, and T. M. Duman, "Over-the-air federated learning with energy harvesting devices," in *Proc. IEEE Glob. Commun. Conf.* IEEE, 2022, pp. 1942–1947.
- [27] S. Wan, J. Lu, P. Fan, Y. Shao, C. Peng, and K. B. Letaief, "Convergence analysis and system design for federated learning over wireless networks," *IEEE J. Select. Areas Commun.*, vol. 39, no. 12, pp. 3622–3639, 2021.

- [28] T. Sery, N. Shlezinger, K. Cohen, and Y. C. Eldar, "Over-the-air federated learning from heterogeneous data," *IEEE Trans. Signal Processing*, vol. 69, pp. 3796–3811, 2021.
- [29] Y. Sun, S. Zhou, Z. Niu, and D. Gündüz, "Time-correlated sparsification for efficient over-the-air model aggregation in wireless federated learning," in *Proc. IEEE Int. Conf. Commun.*, May 2022, pp. 1–6.
- [30] M. M. Amiri, T. M. Duman, D. Gündüz, S. R. Kulkarni, and H. V. Poor, "Blind federated edge learning," *IEEE Trans. Wireless Commun.*, vol. 20, no. 8, pp. 5129–5143, 2021.
- [31] X. Wei, C. Shen, J. Yang, and H. V. Poor, "Random orthogonalization for federated learning in massive MIMO systems," in *Proc. IEEE Int. Conf. Commun.*, 2022, pp. 3382–3387.
- [32] M. Abadi, A. Chu, I. Goodfellow, H. B. McMahan, I. Mironov, K. Talwar, and L. Zhang, "Deep learning with differential privacy," in *Proc. ACM Conf. Comput. Commun. Secur.*, 2016, pp. 308–318.
- [33] J. Du, S. Li, X. Chen, S. Chen, and M. Hong, "Dynamic differential-privacy preserving SGD," *arXiv preprint arXiv:2111.00173*, 2021.
- [34] M. van Dijk, P. H. Nguyen, T. N. Nguyen, and L. M. Nguyen, "Generalizing DP-SGD with shuffling and batching clipping," *arXiv preprint arXiv:2212.05796*, 2022.
- [35] X. Zhang, X. Chen, M. Hong, Z. S. Wu, and J. Yi, "Understanding clipping for federated learning: Convergence and client-level differential privacy," in *Proc. International Conference on Machine Learning*, 2022.
- [36] G. Andrew, O. Thakkar, B. McMahan, and S. Ramaswamy, "Differentially private learning with adaptive clipping," *Advances in Neural Information Systems*, vol. 34, pp. 17 455–17 466, 2021.
- [37] B. Balle, G. Barthe, and M. Gaboardi, "Privacy amplification by subsampling: Tight analyses via couplings and divergences," *Advances in Neural Information Systems*, vol. 31, 2018.
- [38] B. Hasircioğlu and D. Gündüz, "Private wireless federated learning with anonymous over-the-air computation," in *IEEE Int. Conf. Acoust. Speech Signal Process.*, 2021, pp. 5195–5199.
- [39] N. Agarwal, A. T. Suresh, F. X. X. Yu, S. Kumar, and B. McMahan, "cpSGD: Communication-efficient and differentially-private distributed SGD," *Advances in Neural Information Systems*, vol. 31, 2018.
- [40] V. Gandikota, D. Kane, R. K. Maity, and A. Mazumdar, "vpSGD: Vector quantized stochastic gradient descent," in *AISTATS*. PMLR, 2021, pp. 2197–2205.
- [41] K. Wei, J. Li, M. Ding, C. Ma, H. H. Yang, F. Farokhi, S. Jin, T. Q. Quek, and H. V. Poor, "Federated learning with differential privacy: Algorithms and performance analysis," *IEEE Trans. Inf. Forensics Secur.*, vol. 15, pp. 3454–3469, 2020.
- [42] M. Seif, R. Tandon, and M. Li, "Wireless federated learning with local differential privacy," in *IEEE Int. Symp. Inf. Theory*, 2020, pp. 2604–2609.
- [43] D. Liu and O. Simeone, "Privacy for free: Wireless federated learning via uncoded transmission with adaptive power control," *IEEE J. Select. Areas Commun.*, vol. 39, no. 1, pp. 170–185, 2020.
- [44] S. Yang and Y. Liu, "Differentially private federated learning in multi-cell networks," in *IEEE/CIC ICC*, 2021, pp. 53–58.
- [45] R. Hu, Y. Guo, H. Li, Q. Pei, and Y. Gong, "Personalized federated learning with differential privacy," *IEEE Internet Things J.*, vol. 7, no. 10, pp. 9530–9539, 2020.
- [46] K. Wei, J. Li, C. Ma, M. Ding, C. Chen, S. Jin, Z. Han, and H. V. Poor, "Low-latency federated learning over wireless channels with differential privacy," *IEEE J. Select. Areas Commun.*, vol. 40, no. 1, pp. 290–307, 2021.
- [47] M. Kim, O. Günlü, and R. F. Schaefer, "Federated learning with local differential privacy: Trade-offs between privacy, utility, and communication," in *IEEE Int. Conf. Acoust. Speech Signal Process.*, 2021, pp. 2650–2654.
- [48] S. Sesia, I. Toufik, and M. Baker, *LTE - The UMTS Long Term Evolution: From Theory to Practice*, 2nd ed. Wiley, 2011.

- [49] N. S. Pillai and X.-L. Meng, “An unexpected encounter with Cauchy and Lévy,” *The Annals of Statistics*, vol. 44, no. 5, pp. 2089–2097, 2016.
- [50] T. Sery and K. Cohen, “On analog gradient descent learning over multiple access fading channels,” *IEEE Trans. on Signal Processing*, vol. 68, pp. 2897–2911, 2020.
- [51] X. Wei, C. Shen, J. Yang, and H. V. Poor, “Random orthogonalization for federated learning in massive MIMO systems,” 2022. [Online]. Available: <https://arxiv.org/abs/2201.12490>
- [52] I. Mironov, “Rényi differential privacy,” in *IEEE Computer Security Foundations Symposium*, 2017, pp. 263–275.
- [53] I. Mironov, K. Talwar, and L. Zhang, “Rényi differential privacy of the sampled gaussian mechanism,” *arXiv preprint arXiv:1908.10530*, 2019.
- [54] O. Goldreich, “Secure multi-party computation,” 1998.
- [55] W. Du and M. J. Atallah, “Secure multi-party computation problems and their applications: a review and open problems,” in *Proc. Workshop on New Security Paradigms*, 2001, pp. 13–22.
- [56] W. Diffie and M. E. Hellman, “New directions in cryptography,” in *Democratizing Cryptography: The Work of Whitfield Diffie and Martin Hellman*, 2022, pp. 365–390.
- [57] X. Li, K. Huang, W. Yang, S. Wang, and Z. Zhang, “On the convergence of FedAvg on non-IID data,” in *International Conference on Learning Representations*, 2020.
- [58] P. Jiang and G. Agrawal, “A linear speedup analysis of distributed deep learning with sparse and quantized communication,” in *Advances in Neural Information Processing Systems*, 2018, pp. 2525–2536.
- [59] S. U. Stich, “Local SGD converges fast and communicates little,” in *International Conference on Learning Representations*, 2018.
- [60] S. Zheng, C. Shen, and X. Chen, “Design and analysis of uplink and downlink communications for federated learning,” *IEEE J. Select. Areas Commun.*, vol. 39, no. 7, pp. 2150–2167, July 2021.
- [61] M. Bun and T. Steinke, “Concentrated differential privacy: Simplifications, extensions, and lower bounds,” in *Proc. Theory of Cryptography Conference*. Springer, 2016, pp. 635–658.
- [62] T. Van Erven and P. Harremoës, “Rényi divergence and kullback-leibler divergence,” *IEEE Trans. Inf. Theory*, vol. 60, no. 7, pp. 3797–3820, 2014.
- [63] H. Mania, X. Pan, D. Papailiopoulos, B. Recht, K. Ramchandran, and M. I. Jordan, “Perturbed iterate analysis for asynchronous stochastic optimization,” *SIAM Journal on Optimization*, vol. 27, no. 4, pp. 2202–2229, 2017.
- [64] S. Nadarajah and S. Kotz, “A truncated Cauchy distribution,” *International Journal of Mathematical Education in Science and Technology*, vol. 37, no. 5, pp. 605–608, 2006.